



MULTIPLEXING IMMUNOASSAY FOR THE DIAGNOSIS
OF ACUTE KIDNEY INJURY

MISS THANAPORN BOVORNVIRAKIT

A THESIS SUBMITTED IN PARTIAL FULFILLMENT
OF THE REQUIREMENTS FOR
THE DEGREE OF MASTER OF SCIENCE (BIOLOGICAL ENGINEERING)
FACULTY OF ENGINEERING
KING MONGKUT'S UNIVERSITY OF TECHNOLOGY THONBURI
2011

Multiplexing Immunoassay for the Diagnosis
of Acute Kidney Injury

Miss Thanaporn Bovornvirakit B.Sc. (Biotechnology)

A Thesis Submitted in Partial Fulfillment
of the Requirement for
the Degree of Master of Science (Biological Engineering)
Faculty of Engineering
King Mongkut's University of Technology Thonburi
2011

Thesis Committee

..... (Asst. Prof. Diew Koolpiruck, Ph.D.)	Chairman of Thesis Committee
..... (Asst. Prof. Kwanchanok Pasuwat, Ph.D.)	Member and Thesis Advisor
..... (Asst. Prof. Teeranoot Chanthasopeephan, Ph.D.)	Member
..... (Assoc. Prof. Yingyos Aviningsanon, M.D.)	Member

Copyright Reserved

Thesis Title	Multiplexing Immunoassay for the Diagnosis of Acute Kidney Injury
Thesis Credits	12
Candidate	Miss Thanaporn Bovornvirakit
Thesis Advisor	Asst. Prof. Dr. Kwanchanok Pasuwat
Program	Master of Science
Field of Study	Biological Engineering
Faculty	Engineering
B.E.	2554

Abstract

Acute kidney injury (AKI) previously known as acute renal failure (ARF) is becoming a new worldwide public health problem. A diagnosis of this disease using serum creatinine is still a problem in clinical practice due to the insensitivity of the technique. Therefore, a measurement of biomarkers responsible for AKI has received much attention in the past couple of years. Neutrophil gelatinase-associated lipocalin (NGAL) and cytokine interleukin-18 (IL-18) were reported as two of the early biomarkers for AKI. The most commonly used method to detect these biomarkers is an immunoassay. This study used a planar platform (microscope slide) instead of a well-based platform to perform an immunoassay using fluorescence for detection. The advantages of the planar platform include lower reagent consumption, simplicity, and cost-effectiveness. In this study, anti-human IL-18 antibody and anti-human NGAL antibody were immobilized onto a microscope slide using a covalent binding method. The system was used to perform a sandwich immunoassay to detect the concentrations of IL-18 and NGAL present in the sample. Make-up samples were diluted at the concentration between 10 to 1000 pg/ml for IL-18 and 10 to 1000 ng/ml for NGAL to create a calibration curve. The precision of the system was determined using the coefficient of variability (CV), which was found to be less than 10%. This result indicates that this system is highly reproducible. The plasma samples of patients with AKI and healthy controls were tested for IL-18 and NGAL content using the glass slide system via the multiplexing immunoassay technique. The performance of this immunoassay system was compared with that of the Enzyme-Linked Immuno-Sorbent Assay (ELISA) to determine the diagnostic accuracy of this system. It was found that the measurements from both systems were statistically similar.

Keywords: Acute Kidney Injury/ Multiplexing Immunoassay/ Interleukin-18/
Neutrophil Gelatinase-associated Lipocalin

หัวข้อวิทยานิพนธ์	การวินิจฉัยโรคไตวายเฉียบพลันโดยใช้เทคโนโลยี Multiplexing Immunoassay
หน่วยกิต	12
ผู้เขียน	นางสาวชนภรณ์ บวรวิริกิจ
อาจารย์ที่ปรึกษา	ผศ. ดร. ขวัญชนก พสุวัต
หลักสูตร	วิทยาศาสตรมหาบัณฑิต
สาขาวิชา	วิศวกรรมชีวภาพ
คณะ	วิศวกรรมศาสตร์
พ.ศ.	2554

บทคัดย่อ

โรคไตวายเฉียบพลัน เป็นปัญหาด้านสุขภาพที่สำคัญทั่วโลก ปัจจุบันการวินิจฉัยโรคนี้ในทางคลินิกทำได้โดย ดูการเปลี่ยนแปลงค่า เซรั่มครีเอตินิน (serum creatinine) ในเลือดแต่วิธีนี้ยังมีข้อเสียอยู่เนื่องจาก กบัจจายที่ส่งผลต่อค่า รเปลี่ยนแปลงค่า เซรั่มครีเอตินิน มีหลายปัจจัย เช่น น้ำหนัก อายุ เพศ โภชนาการ เป็ นต้น ซึ่งปัจจัยเหล่านี้ ไม่ได้เกี่ยวข้องกับโดยตรงกับไต ทำให้ผู้ป่วยไม่ได้รับการรักษาที่ทันท่วงที ดังนั้นในช่วงสองสามปีที่ผ่าน มา ตัวบ่งชี้ทางชีวภาพ จึงเข้ามามีบทบาทที่สำคัญ งานวิจัยจำนวนมากได้ ระบุว่าตัวบ่งชี้ทางชีวภาพสำหรับโรคไตวายเฉียบพลันมีหลายชนิด โดยneutrophil gelatinase-associated lipocalin (NGAL) และ interleukin-18 (IL-18) เป็นตัวบ่งชี้ทางชีวภาพ สำหรับโรคไตวายเฉียบพลันด้วย เนื่องจาก มีงานวิจัย ได้รายงานว่ ทั้ง IL-18 และ NGAL สามารถตรวจวัดการเปลี่ ยนแปลงได้ล่วงหน้า ก่ อนที่ผู้ป่วยจะมีอาการไตวายเกิดขึ้น วิธีการตรวจวัดปริมาณ ที่ตัวบ่งชี้ทางชีวภาพ นิยมมากที่สุด คือ เทคนิค immunoassay งานวิจัยนี้ได้พัฒนา รูปแบบการทำ immunoassay เป็นแบบ ระนาบ (planar platform) โดยใช้สไลด์แก้ว (microscope glass slide) เป็นพื้นผิววัสดุและ ใช้สารเรืองแสง (fluorescence) สำหรับการตรวจสอบ ข้อดีของ แพลตฟอร์มระนาบ นี้ คือ ปริมาณการใช้ สารที่น้อยมากและมีประสิทธิภาพการตรึงแอนติ บอดีที่ดีกว่า ในการศึกษานี้ แอนติบอดีที่จำเพาะต่อ IL-18 และ NGAL จะถูกตรึงบน สไลด์โดยใช้วิธีโควาเลนต์ (covalent binding) โปรตีนทั้งสองชนิด จะ ถูกถูกเจือจางที่ความเข้มข้นต่างกัน (10-1000 pg/ml สำหรับ IL-18 และ 10-1000 ng/ml สำหรับ NGAL) เพื่อสร้าง กราฟมาตรฐาน ในการหา ปริมาณ ความน่าเชื่อถือของระบบ นี้ถูกกำหนดโดยใช้ ค่าสัมประสิทธิ์ของความแปรปรวน (CV) พบว่ามีค่าน้อยกว่า 10% ซึ่งเป็นค่าที่ยอมรับ ในงานวิจัย ตัวอย่างพลาสมา ของผู้ป่วย ไตวายเฉียบพลัน และคนปกติถูกนำมาวิเคราะห์หาปริมาณ IL-18 และ NGAL ซึ่งทดสอบบนสไลด์แก้ว

โดยใช้เทคนิค Multiplexing Immunoassay และเปรียบเทียบ ประสิทธิภาพของระบบนี้ เมื่อเทียบกับ การหาปริมาณโปรตีน 2 ชนิด โดยใช้วิธี Enzyme-Linked Immuno-Sorbent Assay (ELISA) เพื่อดูความแม่นยำของวิธีวิเคราะห์จากสไลด์แก้ว ผลการทดลองที่ได้พบว่า ปริมาณโปรตีนทั้ง 2 ชนิด ที่วัดได้จากทั้ง 2 ระบบ มีค่าใกล้เคียงกัน ในทางสถิติ

คำสำคัญ : โรคไตวายเฉียบพลัน/ Multiplexing Immunoassay/ Interleukin-18/ Neutrophil Gelatinase-associated Lipocalin

ACKNOWLEDGEMENTS

Foremost, I would like to express my deepest gratitude to my advisor Asst. Prof. Dr. Kwanchanok Pasuwat for her patience, helpful suggestion, continuous support, and useful advice over the period of this thesis. I would have been lost without her.

Besides my advisor, I would like to record my gratitude to Dr. Dujduan Waraho and my thesis committee: Asst. Prof. Dr. Diew Koolpiruck, Asst. Prof. Dr. Teeranoot Chanthasopeephan, and Assoc. Prof. Yingyos Avihingsanon, for their insightful comments, and hard questions.

I would also like to specially thank Assoc. Prof. Yingyos Avihingsanon, Dr. Khajohn Tiranathanagul, and staffs at King Chulalongkorn Memorial Hospital for patient plasma samples and their kind assistance.

I am very thankful to many people at MTEC, Biosensor Technology Laboratory (KMUTT), and Algal Biotechnology Laboratory (KMUTT) who support in helping me, in particular, with laboratory equipment.

I thank my fellow labmates at Biological Engineering Laboratory (KMUTT) and friends for advice, the stimulating discussions, and great morale.

I am grateful to thank the financial support from the Higher Education Research Promotion and National Research University (NRU) Project of Thailand by Office of the Higher Education Commission and also National Research Council of Thailand (NRCT).

Lastly, I wish to thank my family for supporting me spiritually throughout my life and providing a loving environment for me.

CONTENTS

	PAGE
ENGLISH ABSTRACT	ii
THAI ABSTRACT	iii
ACKNOWLEDGEMENTS	v
CONTENTS	vi
LIST OF TABLES	ix
LIST OF FIGURES	x
LIST OF TECHNICAL VOCABULARY AND ABBREVIATIONS	xii
LIST OF EQUATIONS	xiii
CHAPTER	
1.INTRODUCTION	1
1.1 Motivation	1
1.2 Objective	1
1.3 Scope of study	2
1.4 Contribution	2
2.LITERATURE REVIEW	3
2.1 Acute kidney injury	3
2.1.1 Diagnosis	4
2.2 Biomarker of acute kidney injury	4
2.2.1 Neutrophil gelatinase-associated lipocalin	5
2.2.2 Interleukin-18	5
2.2.3 Other biomarkers	6
2.3 Immunoassay	6
2.4 Multiplexing immunoassay	7
2.4.1 Solid support	8
2.4.2 Antibody immobilization	8
2.4.3 Applications	11
3.MATERIALS AND METHODS	13
3.1 Materials	13
3.3 Cleaning glass slide	13
3.4 Surface Modification	13

3.5 Antibody Immobilization	13
3.6 Immunoassay	14
3.7 Enzyme-Linked Immunosorbent Assay	14
3.7.1 NGAL	14
3.7.2 Interleukin-18	14
4.RESULTS AND DISCUSSIONS	15
4.1 Measurement of contact angles	15
4.2 Surface Modification & Antibody Immobilization	16
4.3 The efficiency of the concentration of linker to immobilize antibody	17
4.4 Neutrophil gelatinase-associated lipocalin (NGAL)	18
4.4.1 Optimized capture anti-NGAL antibody	18
4.4.2 Calibration curve NGAL	19
4.4.3 Reliability assay	20
4.4.4 Comparison between ELISA and slide	21
4.5 Interleukin-18 (IL-18)	21
4.5.1 Optimized capture anti-IL-18 antibody	21
4.5.2 Calibration curve	22
4.5.3 Reliability assay	24
4.5.4 Comparison between ELISA and slide	24
4.6 Cross-reactivity	24
4.7 Analysis of plasma samples	25
4.8 Comparison between glass slide system and ELISA	25
4.9 Preservation of the immobilized antibody	28
4.9.1 The effect of temperature to immobilized slide	28
4.9.2 The effect of humidity to immobilized slide	29
4.9.3 The effect of oxygen to immobilized slide	31
4.10 Influence of incubation time on signal intensity	32
5. CONCLUSIONS	35
5.1 Conclusions	35
5.2 Recommendations	35
REFERENCES	37
APPENDIX	
A. The data of NGAL and IL-18	39
B. Microfluidic study	53

C. Consent form	57
CURRICULUM VITAE	59

LIST OF TABLES

TABLE	PAGE
2.1 Proposed classification scheme for acute kidney injury (AKI) in patients[10]	4
2.2 Surface designs of solid supports (Modified from[6])	8
2.3 Slide chemistries available for antibody immobilization [23, 24]	12
4.1 Water contact angles of Piranha cleaning, modified - and immobilized antibody glass surfaces	16
4.2 The concentration of the solution between EDC and antibody	16
4.3 The concentration of the solution between EDC, NHS and antibody	16
4.4 The concentration of the solution between EDC, NHS and antibody	17
4.5 Intra- and Inter-assay of NGAL	20
4.6 Comparison between ELISA and glass slide of NGAL	21
4.7 Intra- and Inter-assay of IL-18	24
4.8 Comparison between ELISA and glass slide of IL-18	24
4.9 Plasma NGAL (ng/ml) and IL-18 (pg/ml) obtained by glass slide system	25
4.10 The levels of NGAL and IL-18 obtained by glass slide and ELISA	26
4.11 The condition for keeping immobilized slide	28
4.12 The incubation time of each step	32
A.1 Mean fluorescence intensity, standard deviation and %of standard deviation of calibration curve of NGAL	43
A. 2 Mean fluorescence intensity, standard deviation and %of standard deviation of calibration curve of IL-18	43
A.3 Fluorescence intensity and absorbance obtained by glass slide system ELISA method for NGAL detection	45
A.4 Fluorescence intensity and absorbance obtained by glass slide system ELISA method for IL-18 detection	47
A.5 Quantitative of plasma NGAL (ng/ml) obtained by glass slide system and ELISA method	49
A.6 Quantitative of plasma IL-18 (pg/ml) obtained by glass slide system and ELISA method	51

LIST OF FIGURES

FIGURE	PAGE
2.1 Structure of kidney	3
2.2 Mechanisms of acute kidney injury [9]	4
2.3 Biomarkers for early diagnostic of acute kidney injury (AKI)[4]	5
2.4 (a) a homogeneous competitive immunoassay, (b) a heterogeneous non-competitive immunoassay, (c) a heterogeneous competitive immunoassay and (d) a heterogeneous competitive immunometric assay [23]	7
2.5 Signal and signal density in microspots[7]	8
2.6 The structure of antibody	9
2.7 Silanization	10
2.8 Surface functionalization, antibody activation and antibody immobilization on a cantilever's sensing surface. (I) Cleaning protocol; (II) silanylation; (IIa) activation of carboxylic groups on antibody; (III) antibody coupling to surface amines [34].	10
2.9 Avidin-biotin system	11
3.1 Design	14
4.1 Water contact angle image	15
4.2 Structures of EDC and NHS	16
4.3 Bar plots between rabbit IgG concentration and fluorescence intensity	17
4.4 Bar plot between fluorescence intensity and antibody concentration	18
4.5 Optimized capture anti-NGAL antibody	18
4.6 A. The location of each concentration of NGAL	19
4.7 Calibration curve of NGAL	20
4.8 Fluorescence intensities when the concentrations of immobilized antibody specific for IL-18 were 2, 5, and 10 $\mu\text{g/mL}$	22
4.9 A. The location of each concentration of IL-18	23
4.10 Calibration curve of IL-18	23
4.11 Cross reactivity experiment	25
4.12 Scatter plots showing the linear relationship between the gold standard ELISAs and the fluorescence scanner of NGAL	27
4.13 Scatter plots showing the linear relationship between the gold standard ELISAs and the fluorescence scanner of IL-18	27
4.14 The effect of temperature to stability of immobilized anti-human NGAL antibody slide at room temperature (RT) and 4°C in various NGAL concentrations	28
4.15 The stability of immobilized anti-human IL-18 antibody slide at room temperature (RT) and 4°C in various IL-18 concentrations	29
4. 16 The effect of humidity to stability immobilized anti-human NGAL antibody slide with and without humidity (H, WH) in various NGAL concentrations	30
4.17 The effect of humidity to stability immobilized anti-human IL-18 antibody slide with and without humidity (H, WH) in various IL-18 concentrations	30
4.18 The effect of oxygen to stability immobilized anti-human NGAL antibody slide with and without oxygen (O, WO) in various NGAL concentrations	31

4. 19	The effect of oxygen to stability of immobilized anti-human IL-18 antibody slide with and without oxygen (O, WO) in various IL-18 concentrations	32
4.20	The effect of incubation time to assay in NGAL protein	33
4. 21	The effect of incubation time to assay in IL-18 protein	34
A.1	The graph of NGAL at 100-10,000 ng/ml	43
A.2	Spot morphology	44
B.1	Oxygen plasma treat	54
B.2	Fluorescence image A. non-oxygen plasma treat and	54
B.3	Evacuated the air in PDMS	55
B.4	Power free testing of each micro chip	56

LIST OF TECHNICAL VOCABULARY AND ABBREVIATIONS

AKI	=	Acute Kidney Injury
ARF	=	Acute Renal Failure
NGAL	=	Neutrophil Gelatinase-Associated Lipocalin
IL-18	=	Interleukin-18
ELISA	=	Enzyme Linked Immunosorbent Assay
MIA	=	Multiplexing Immunoassay
ICU	=	Intensive Care Unit
RIFLE	=	Risk of kidney dysfunction, Injury to the kidney, Failure of kidney function, Loss of kidney function, and End-stage kidney disease
GFR	=	Glomerular Filtration Rate
SCr	=	Serum Creatinine;
RRT	=	Renal Replacement Therapy
LCN2	=	Lipocalin-2
ARDS	=	Acute Respiratory Distress Syndrome
IL-6	=	Interleukin-6
KIM-1	=	Kidney injury molecule-1
BUN	=	Blood Urea Nitrogen
mm	=	Millimeter
cm ²	=	Centimeter Squared
μL	=	Microliter
NHS	=	<i>N</i> -hydroxysuccinimide
APTES	=	3-aminopropyltriethoxysilane
GA	=	Glutaraldehyde
EDC	=	1-ethyl-3-(3-dimethylaminopropyl) carbodiimide hydrochloride
BSA	=	Bovine serum albumin

LIST OF EQUATIONS

EQUATION		PAGE
4.5.3.1	The coefficient of variable	20
4.5.3.2	The percentage of error	21

CHAPTER 1 INTRODUCTION

1.1 Motivation

Acute kidney injury (AKI) or acute renal failure (ARF) is characterized by a deterioration of renal function over a period of hours to days. AKI results in failure of the kidney to excrete nitrogenous waste products and to maintain fluid and electrolyte homeostasis [1]. The mortality and morbidity rate of hospitalized patients with acute kidney injury has increased in recent years and become a worldwide public health problem [2]. The major reason is the lack of early diagnosis of AKI. Current diagnosis of AKI relies on the evaluation of the levels of serum creatinine, urea, blood urea nitrogen levels and urinalysis changes which have limited [3]. All of those methods are insensitive, nonspecific, and change significantly [4]. Therefore, the biomarkers come to play a more important role. There are many researches report about the biomarkers responsible for AKI. Neutrophil Gelatinase-Associated Lipocalin (NGAL) and Cytokine interleukin-18 (IL-18) have been reported as the early biomarker for AKI. The measurement of those biomarkers is currently done by automated assays usually via enzyme-linked immunosorbent assay (ELISA). However, the traditional methods have limited. Although ELISA provides precise and accurate results, it requires large amount of reagent and is time-consuming, labor-intensive, and unable to produce results simultaneously [4,5].

Among the various methods currently available, multiplexing immunoassay (MIA) technology has promising advantages. The principle of this technology is based on an antigen and its corresponding antibody to recognize each other and form a complex due to their specific affinity. This technology allows rapid, miniaturized, sensitive, simultaneous and multiplex detection [6]. According to Ekins' theory describing molecule interaction, miniaturization leads to an increase in detection sensitivity. Only a small amount of analyte molecules will be captured on to a spot that only contains a minute amount of immobilized capture molecules. The formation of antigen-antibody complexes will not change significantly even though the capture molecule is a high affinity binder and the analyte concentration is low. Therefore, the analyte molecules captured in the spot directly reflect the analyte concentration in the sample [7,8].

Thus, the aim of this work is to develop the multiplexing immunoassay to analyze the healthy control and patient samples, specifically plasma samples, for diagnosis of AKI. The specific antibody for NGAL and IL-18 were immobilized on glass slides with a covalent binding method and detected with fluorescence spectroscopy. The reliability of assay is determined with the coefficient of variables. The performance of the immunoassay on the modified glass slide is compared with the conventional method (ELISA).

1.2 Objective

1. To fabricate a prototype of immunoassay on a glass slide to detect NGAL and IL-18 by using a glass slide as a solid support and fluorescence detection.
2. To test the multiplexing immunoassay against a conventional technology for example, ELISA.
3. To verify the efficiency of the multiplexing immunoassay when tested with plasma samples of healthy control and patient with AKI.

1.3 Scope of study

1. To determine the optimum conditions in antibody concentration and time to immobilize the antibodies on glass surface.
2. To detect 2 biomarkers of AKI disease: NGAL and IL-18, from plasma samples with multiplexing immunoassay.
3. To evaluate the reliability of assay with intra- and inter-assay method

1.4 Contribution

Multiplexing immunoassay is capable of analyzing 2 biomarkers of kidney disease from samples of patients.

CHAPTER 2 LITERATURE REVIEW

2.1 Acute kidney injury

Kidneys are important organs which are located on each side of spine above waist. The main functions of kidney are the production of urine by filtering waste products from your blood and the excretion of water soluble waste products of metabolism. Moreover, they control the balance of salt and water in body, produce and regulate hormone such as erythropoietin and renin, and help regulate blood pressure.

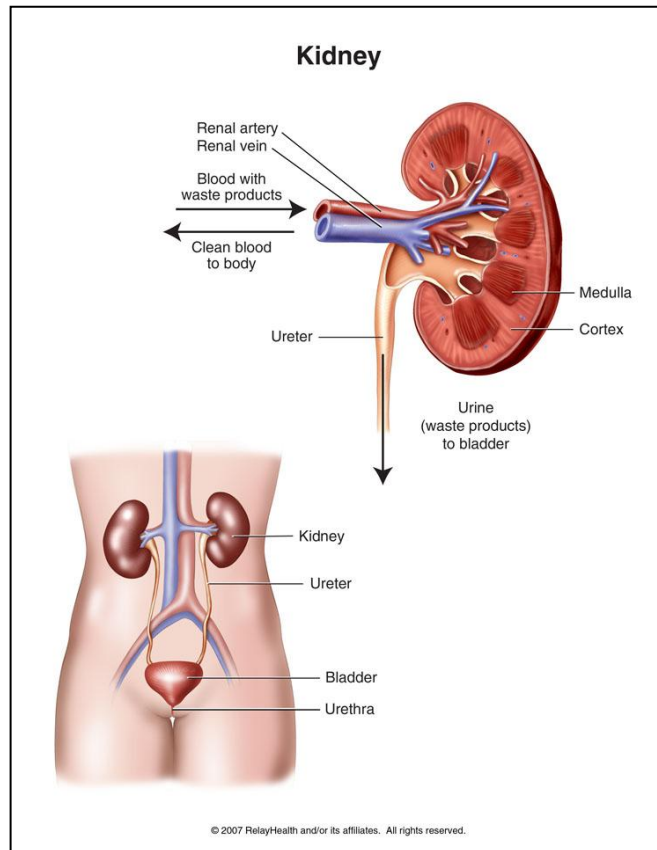


Figure 2.1 Structure of kidney

Acute kidney injury (AKI), also generally known as acute renal failure (ARF), describes a rapid loss of kidney function. Its causes are numerous and include low blood volume, ischemia, exposure to toxins, and urinary obstruction (e.g. prostate enlargement). The patients who most risk for AKI are surgery, intensive care unit (ICU) and chronic disease (diabetes). The mechanisms involved in the etiology of AKI are endothelial injury from vascular perturbations and formation of inflammatory mediators (Figure 2.2).

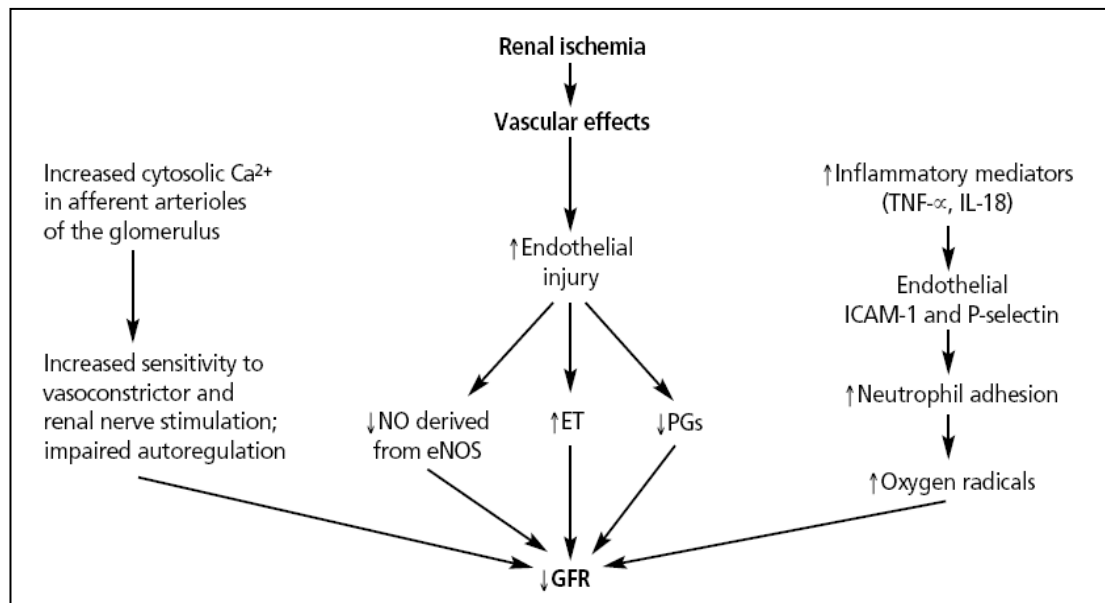


Figure 2.2 Mechanisms of acute kidney injury [9]

2.1.1 Diagnosis

Current diagnosis of AKI relies on elevations in the levels of serum creatinine, urea, BUN, and urinalysis changes, which is poor sensitivity and specificity. The concentration of serum creatinine does not increase until about half of the kidney function is lost. Recently, RIFLE criteria (risk of kidney dysfunction, injury to the kidney, failure of kidney function, loss of kidney function, and end-stage kidney disease), that based on glomerular filtration rate (serum creatinine increase) and weight-dependent urine output, have been used to diagnose AKI (Table 2.1) [9].

Table 2.1 Proposed classification scheme for acute kidney injury (AKI) in patients [10]

RIFLE classification	Creatinine/GFR criterion	Urine output criterion
Risk	SCr increase x 1.5 or GFR reduction > 25%	Dieresis < 0.5ml/kg/h in 6h
Injury	SCr increase x 2 or TFG reduction > 50%	Dieresis < 0.5ml/kg/h in 12h
Failure	SCr increase x 3 or GFR reduction > 25% or SCr > 4mg/dl	Dieresis < 0.3ml/kg/h in 24h or anuria for 12h
Loss	Completely loss renal function > 4 weeks	
End-stage kidney disease	RRT needed > 3 months	

RIFLE – Risk Injury Failure Loss Eng; GFR – glomerular filtration rate; SCr - serum creatinine; RRT – renal replacement therapy

2.2 Biomarker of acute kidney injury

Although serum creatinine is typically used for diagnosis of AKI, it is an insensitive and unreliable biomarker during acute changes in kidney function [11]. The serum creatinine concentration does not increase until about half of the kidney function is lost. Therefore, a measurement of biomarker has come to be a play role. A biomarker can be

any parameter of a patient that can be quantitated. Accessible markers of AKI can be components of serum or urine. Desirable characteristics of AKI biomarkers include: (a) noninvasive and easily detectable in accessible samples such as blood or urine, (b) rapidly and reliably measurable, (c) highly sensitive and specific for AKI, (d) able the identification of AKI subtypes and etiologies, (e) capable of early detection, (f) unaffected by other biological variables, and (g) inexpensive [12,13]. The urine has yielded the most promising markers for the early detection of AKI. However, several other biomarkers have shown promise in diagnosis of AKI.

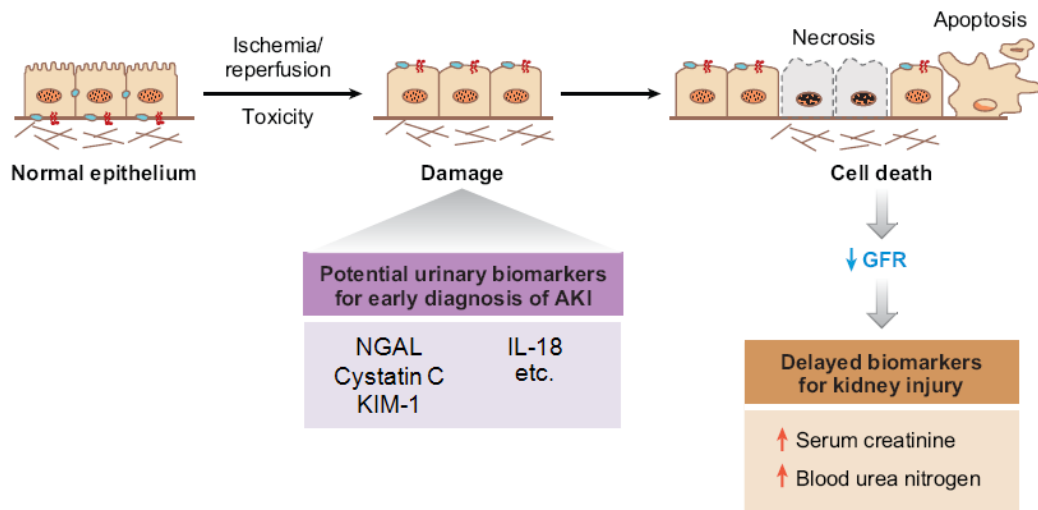


Figure 2.3 Biomarkers for early diagnostic of acute kidney injury (AKI)[4]

2.2.1 Neutrophil gelatinase-associated lipocalin

Neutrophil gelatinase-associated lipocalin (NGAL) or Lipocalin-2 (LCN2) is a 25 kDa protein that covalently bound to gelatinase in specific granules of the neutrophil [3,4,14]. Normally, the expression of NGAL is very low in several human tissues such as kidney, lungs, stomach, uterus, prostate, salivary gland, trachea, and colon [15]. Nevertheless, renal expression of NGAL is increased after ischemic or nephrotoxic injury, and NGAL is released into both urine and plasma. Mishra *et al.* used cDNA microarray assay methods to identify NGAL as a protein strongly expressed in renal tubules in animal models of renal failure. Its expression was increased within few hours [16].

2.2.2 Interleukin-18

Interleukin 18 (IL-18) formerly known as interferon- γ -inducing factor. It is a proinflammatory cytokine that is induced and cleaved as a 24 kDa inactive precursor in the proximal tubule [17]. There was strong marker in the proximal tubules of patients. Elevation was not found in healthy controls or in patients with other renal disease [18].

Parikh *et al.* [19] reported the results of a nested case control study analyzing sequential urine samples from patients enrolled in the Acute Respiratory Distress Syndrome (ARDS) trial. They found that urinary IL-18 levels >100 pg/ml were predictive of AKI developing within 2 days, and correlated with mortality. Later, they used ELISAc to evaluate the level of urinary IL-18 and NGAL from patient with cardiopulmonary bypass and transplantation. Both of IL-18 and NGAL increase.

2.2.3 Other biomarkers

Furthermore, there are many studies to find new biomarker for acute kidney injury. Interleukin-6 is a predominant cytokine in the kidney, and its release is stimulated by tumor necrosis factor- α . IL-6 is a 26 kDa glycoprotein released by T and B lymphocytes, macrophages, fibroblasts, endothelial cells, epithelial cells, mesangial cells, and tubular epithelial cells. It is involved in cell growth and differentiation, including renal tubular epithelial cell regeneration. IL-6 has been implicated in the cascade of cellular events that follows renal ischemic injury [3]. It increases early in the serum of patients with acute kidney injury (AKI). Kidney injury molecule-1 (KIM-1) is a type 1 transmembrane protein that is expressed at very high levels in proximal tubule epithelial cells in human and both mouse and rat kidneys after ischemic or toxic injury [1]. Several studies have been show that KIM-1 was released from cell into urine [20,21]. Thus, it can be detected in the urine. KIM-1 is more sensitivity than serum creatinine and BUN. Cystatin C is a 13 kDa that is important inhibitor of cysteine protease. It is freely filtered by the glomerulus, reabsorbed but not secreted by the proximal tubules [12]. The rise of serum cystatin c is relative with kidney dysfunction. The concentration of cystatin c in human serum is independent of sex, age, and muscle mass. Thus, it is a better marker than serum creatinine.

However, determining these biomarkers simultaneously in the sample is still limitation. Recently, the advance of technologies in the field of proteomics plays more important role to discovery of novel protein biomarkers in renal diseases. Of the various methods currently available, multiplexing immunoassay technology has emerged as the preferred platform.

2.3 Immunoassay

Antibody (Ab) is protein produced in body by immunological responses to the presence of allochthonous substances or antigen (Ag). They have highly specific affinity. Antibody has a unique structure to recognize their specific antigen. This property is the same as a reaction between enzyme and substrate but it is reversible. The sensitivity and specificity of this Ab-Ag interaction allows for the quantification and monitoring of small molecules, such as drugs and metabolites, large proteins, nucleic acids, and pathogens. They have been widely used in clinical analysis, food safety and environmental monitoring, and basic biotechnological investigations.

The immunoassays are widely used in clinical analysis. It can be used to detect the interaction between antibody and antigen. Generally, immunoassays can be classified as either a competitive or a noncompetitive format. In competitive format, the non-labeled antigen and labeled antigen competes binding with limited antibodies. As the amount of unlabeled antigen in a sample increases, the amount of labeled antigens bound to the antibody decreases, resulting in a decrease in the detection signal. The analyte concentration is inversely proportional to the signal. For noncompetitive format, Antigen in a sample conjugate with an excessive amount of Antibody to form a complex that is dependent on the number of Antigen, resulting an increase in the detection signal as the Antigen in the sample increases [22].

Furthermore, immunoassay can also be divided into heterogeneous and homogeneous immunoassay format.

1. Homogeneous immunoassay

In homogeneous immunoassay format (Figure 2.4a), antibodies, antigens and labeled antigens are mixed. The antigens freely marked and those which are linked to the antibodies can be distinguished by a change of activity of the marker when coupled. This platform does not require the antibody or antigen immobilization on a solid substrate.

2. Heterogeneous immunoassay

Antibodies or antigens are immobilized on a solid substrate and form to be immunocomplex with a solution containing the other immunoagent. The non-linked proteins are removed in washing step and the signal obtained from the labels is proportional to the amount of linked protein. The advantage of this format is high surface area/volume ratio and result in good performance in sensitivity. The sandwich immunoassay (Figure 2.4b) and competitive (Figure 2.4c and 2.4d) immunoassay are the most popular methods.[23]

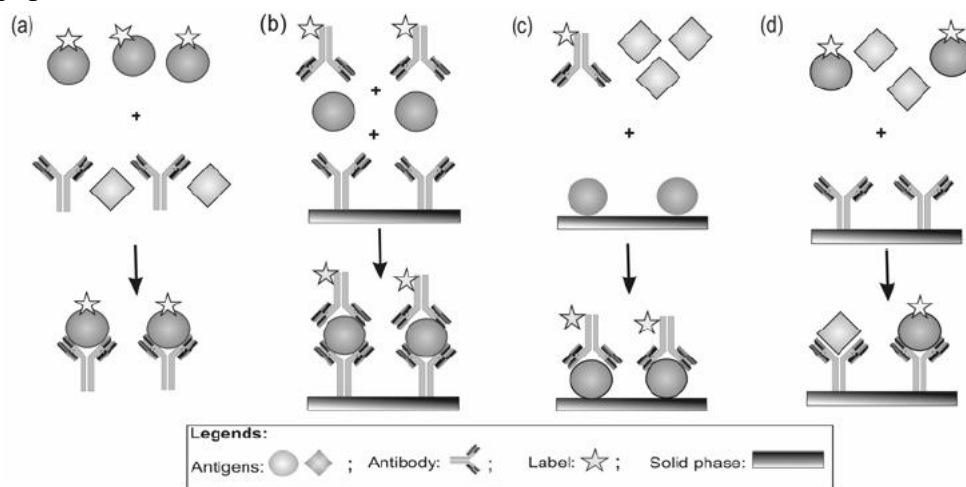


Figure 2.4 (a) a homogeneous competitive immunoassay, (b) a heterogeneous non-competitive immunoassay, (c) a heterogeneous competitive immunoassay and (d) a heterogeneous competitive immunometric assay [23]

2.4 Multiplexing immunoassay

Multiplexing immunoassay are a new powerful proteomic technology that promises to be a powerful tool for multiplexed (simultaneous) analysis of large numbers of substances in a single experiment with consuming only minute amounts of the sample. This technology can be used to generate fast, high-throughput and sensitive assays [6,24]. The concept of this technology is the small amount of antibodies that are immobilized onto a solid substrate and following with blocking step. Blocking step is necessary because it reduces the unspecific binding of analytes and high signal-to-noise ratios can be achieved. This in turn is a prerequisite for higher sensitivity. Then they are incubated with minute amounts of biological sample. Next, antigens-antibodies are detected and quantify, mainly using fluorescence as detection mode. Under ambient analyte conditions, the concentration of analyte in the sample will not change significantly even though the capture molecule is a high affinity binder and the analyte concentration is low (Figure 2.5) [7]. This promising proteomic research tool may provide novel means for early and improved disease diagnostics, observation, predicting relapses and disease recurrence, biomarker discovery, and identification of new improved therapeutics.

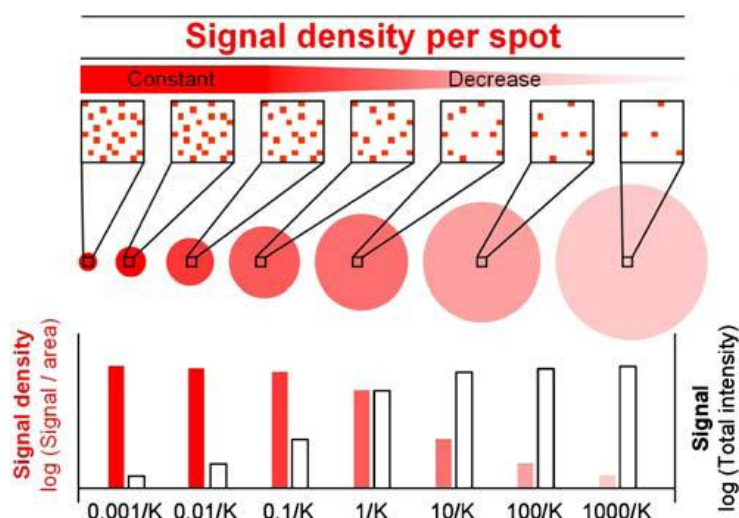


Figure 2.5 Signal and signal density in microspots [7]

2.4.1 Solid support

There are several types of surface designs and materials have been evaluated as a solid supports (Table 2.2). Although plastics have been used for coating antibodies is the most popular but it is not suitable because of its physical, chemical and background fluorescent properties. While fabricated on a microscope slide (glass support) still dominate because glass offers a large variety of different immobilization chemistries.

Table 2.2 Surface designs of solid supports (Modified from [6])

Surface design	Format	Density	Amount of reagent required
Planar solid supports	Microscope slide (75 mm × 25 mm)	High (<5,000/cm ²)	Low to moderate (μL scale or larger)
Well-based	ELISA plates	Moderate (<100/well)	Moderate to high
Micro/nanofluidics	Channels		Low

Recently, solid supports based on predominantly glass-, plastic-, polymer- or silicon slides, often modified with one-, two- or three-dimensional structured surface modifications have been fabricated.

2.4.2 Antibody immobilization

To immobilize antibody onto the surface of substrate, the surface has to be modified to achieve maximum binding capacity. This step is an essential process for the development of most immune-based assay systems. The choice of the immobilization method greatly affects antibody-antigen interactions on the assay surface. The main purposes of immobilization techniques are to enhance the protein activity and not lose the activity of antibody. There are three general methods for antibody immobilization on solid support: (i) physical adsorption, (ii) covalent attachment via reactive groups, and (iii) affinity based interactions between functional groups on the slide and the antibody [25,26].

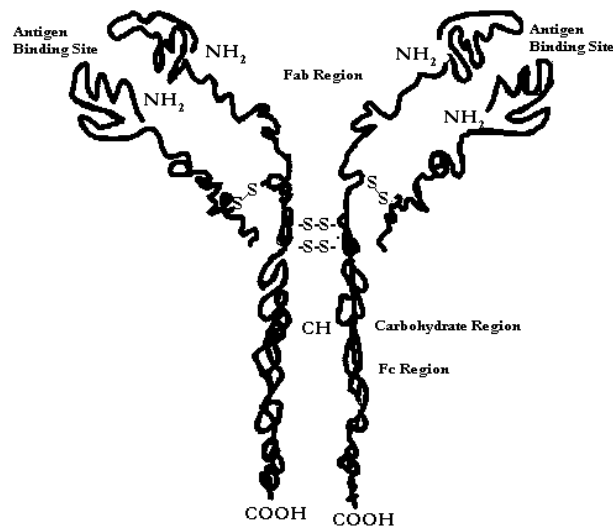


Figure 2.6 the structure of antibody

1. Physical adsorption

The physical adsorption method is the oldest and gentle immobilization method by using mild reaction conditions. It occurs via hydrophilic, hydrophobic, hydrophilic-hydrophobic or ionic interactions between the protein and the solid substrate. Some commonly used slide coatings that can be used to physically adsorb antibodies include agarose, polyacrylamide, nitrocellulose [5], poly-L-lysine [5] or aminosilane [25]. However, adsorbed antibodies are randomly oriented and can lose their antigen binding abilities by denaturation. Moreover, the background signals are generally high. The methods have been used in many applications such as ELISA, multiplexing immunoassay, and immuno-sensors due to their simple procedure (no modifications of antibodies are required) and high antibody-binding capacity. There are several studies to develop the adsorption method to produce proper orientation of antibody like coating the solid surface with calixarene derivatives [26].

2. Covalent Binding

Antibody can be immobilized to the surface by covalent bonds with functional groups on the antibody. (Figure 2.3) such as primary amines in lysines or arginines, reactive thiols in the cysteines in the hinge region or carbohydrates linked the H2 domains of the constant (Fc) region and chemically-activated solid surfaces [25,26]. The covalent binding is the most popular method because amino groups in antibody can bind with several reactive moieties such as aldehyde, epoxy, and *N*-hydroxysuccinimide (NHS) on various solid surfaces. Aldehyde- and epoxy-activated solid substrates have been widely employed as ready-to-use supports for antibody immobilization. Nevertheless, this method is a highly stable process, but covalently-linked antibodies through amino groups are randomly oriented. Although attachment through thiols or carbohydrates allows for directed orientation of antibodies, the protocol for attachment is more complex. The antibody must be treated with chemicals before attachment onto the surfaces such as the disulfide bonds must be reduced or the carbohydrate groups must be oxidized.

For antibody immobilization onto glass substrate, the substrate will be modified the surface to activate surface with organofunctional alkoxy silane such as 3-aminopropyltriethoxysilane (APTES) to form self-assembly of molecules that call silanization. This method is most popular in the field of bionanotechnology [27,28].

The surface of glass has hydroxyl group that can react with the alkoxy groups on the silane by covalent -Si-O-Si- bond (Figure 2.4). Then the linker like homobifunctional cross-linker such as Glutaraldehyde (GA) or heterobifunctional cross-linker such as 1-ethyl-3-(3-dimethylaminopropyl) carbodiimide hydrochloride (EDC) will be used to attach the protein on modified glass's surface [28-34]

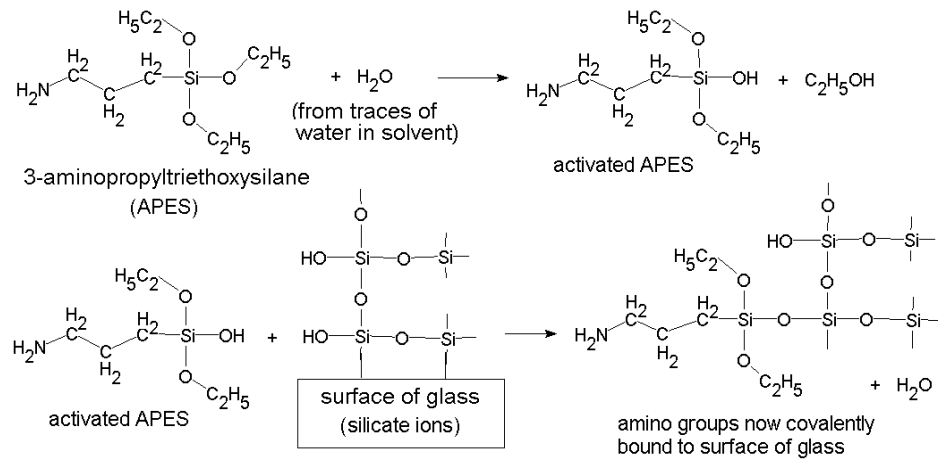


Figure 2.7 Silanization (<http://www.iheworld.com>)

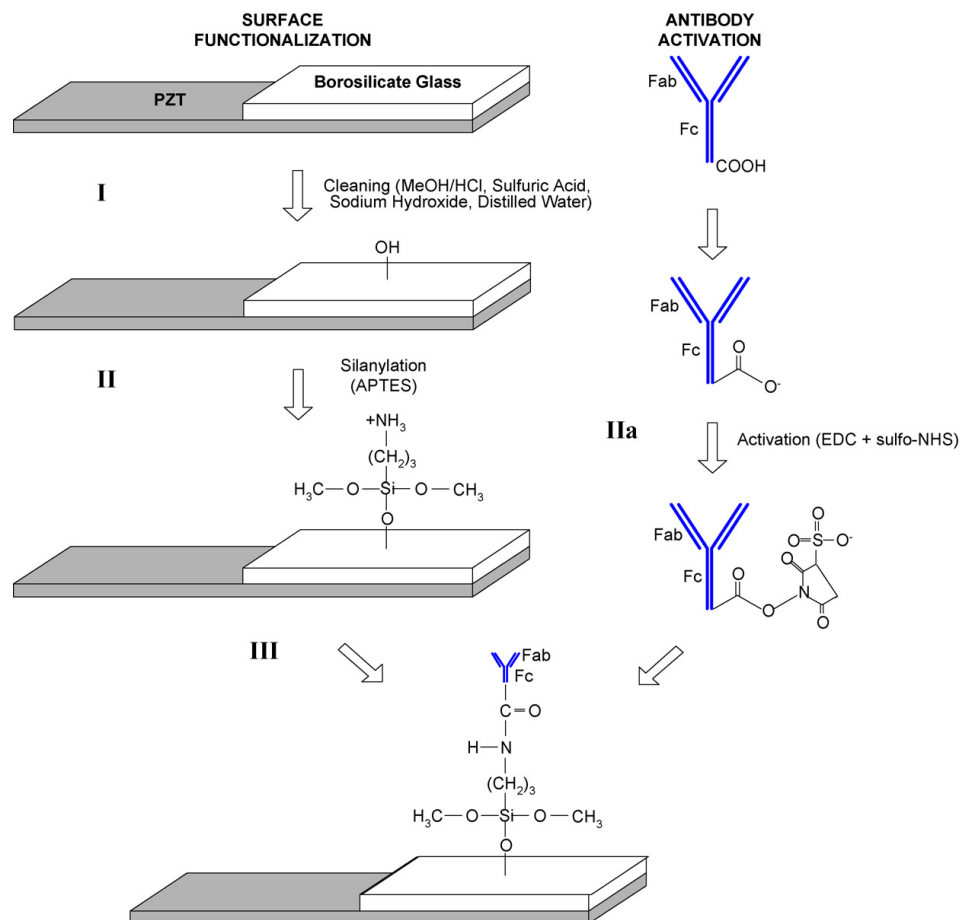


Figure 2.8 Surface functionalization, antibody activation and antibody immobilization on a cantilever's sensing surface. (I) Cleaning protocol; (II) silanylation; (IIa) activation of carboxylic groups on antibody; (III) antibody coupling to surface amines [34].

Hermanson [33] proposed the efficiency protocol for antibody immobilization by using zero-length cross-linker, Carbodiimide hydrochloride (EDC), and N-hydroxysuccinimide (NHS) or N-hydroxysulfosuccinimide (sulfo-NHS). Maraldo and Mutharasan modified this method to detect Bovine serum albumin (BSA) by activation antibody with activating reagent (EDC and sulfo-NHS) and immobilized activated antibody or PZT-glass that was modified surface with silanization (Figure2.5) [34]

3. Affinity Binding

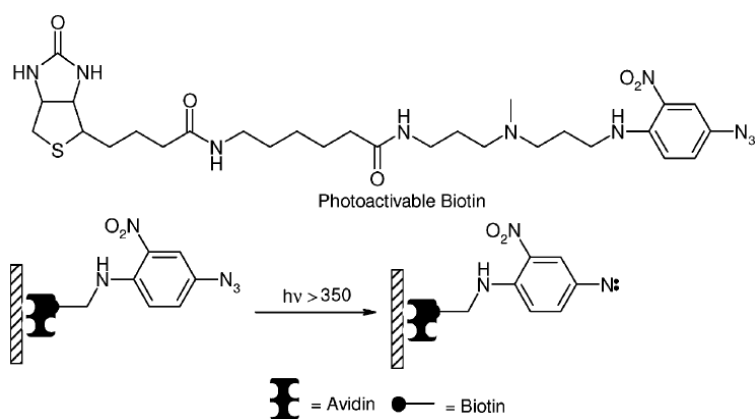


Figure2.9 Avidin-biotin system

The affinity binding method is high specific and selective more than adsorption and covalent. The antibody will be immobilized on protein such as protein G and protein A specifically target the Fc region of an antibody. However, proteins A and G are specific for only certain IgG subclasses and cannot be used universally with all monoclonal antibodies [25].

Furthermore, there are several recombinant antibodies in forms of full-length antibodies, single chain antibody fragments (scFv) or Fab fragments that bind with target were used to immobilize on solid substrate. Using these recombinant antibodies can enhance capacity binding.

All methods have both advantages and disadvantages. Therefore, choice of method and optimization depend on the applications.

2.4.3 Applications

Multiplexing immunoassay can apply with medical, food [5] and environmental. For example, multiplexed assays for cytokines [35-37], allergens [38,39], oncoproteomics [40], drugs and hormones.

However, to my knowledge, there is no evidence to show the application of this novel technology in patients with acute kidney injury for diagnosis.

Table 2.3 Slide chemistries available for antibody immobilization [25,26]

Immobilization Chemistry	Surface Chemistry	Attachment Site	Advantages	Disadvantages
Adsorption	Agarose	Electrostatic Interactions Hydrogen Binding Hydrophobic Interactions	Simple immobilization. No antibody modification. High-level antibody loading.	Random orientation. High background. Antibody denaturation.
	Polyacrylamide			
	Nitrocellulose			
	Poly-L-lysine[41]			
	Amino			
Covalent Binding	Maleimide	Thiol	Simple immobilization. Stable and strong binding of antibody.	Possible pretreatment of antibody required. Potentially random orientation (except thiol and carbohydrate [26]).
	Hydrazine[42]	Carbohydrate		
	Succinimidyl ester[28,34,43,44]	Primary Amine		
	Epoxide			
	Aldehyde			
Affinity Binding	Protein A or G	Fc region	Directed orientation. No antibody modification.	Specific for certain antibody classes and species. Antibody migration. Low specificity. Less stable than covalent immobilization.
	Streptavidin	Biotin		
	Cellulose	Carbohydrate binding molecule		
	Nickel	Histidine tag		
	Nickel-nitrilotriacetic acid			
	Copper			
	Glutathione	GST tag		
	Tag-specific antibody	His, HSV, Myc, and others		

CHAPTER 3 MATERIALS AND METHODS

3.1 Materials

Microscope slides were purchased from Sip Texnet I&E Medical (Sail brand, Jiangsu, China; 25.4 x 76.2 x 1 mm; Cat. 7101). Sodium hydroxide was purchased from Merck. Hydrogenperoxide (H_2O_2) was purchased from Carls Brba. Sulfuric acid (H_2SO_4) was purchased from J.T.Baker. Acetone and sodium hydrogen phosphate (Na_2HPO_4) was purchased from Ajax. 3-aminopropyltriethoxysilane (APTES), succinic acid anhydride (SAA), 1 ethyl-3-(3-dimethylaminopropyl) carbodiimide hydrochloride (EDC) and bovine serum albumin (BSA) were purchased from Sigma. N-hydroxy succinimide (NHS) was purchased from Fluka. Citric acid monohydrate was purchased from Riedel-de Haën. Anti-human IL-18 antibody, recombinant human IL-18, biotin labeled anti-human IL-18 antibody, anti-human NGAL antibody, recombinant human NGAL, biotin labeled anti-human NGAL antibody and northernlightsTM-labeled streptavidin were purchased from R & D Systems (Minneapolis, MN, USA).

3.2 Plasma sample

Plasma samples from patients with AKI were obtained from the King Chulalongkorn Memorial Hospital. Healthy plasma samples were consented from 20 volunteers. The blood samples were collected using heparin tubes. Then, the samples were centrifuged at 2,500 rpm for 5 minutes at room temperature. The Plasma samples were kept at -20°C until use.

3.3 Cleaning glass slide

Glass slides were immersed with 1M NaOH for 20 minutes at room temperature, and thoroughly rinsed with Milli Q and dried under nitrogen flow. After that they were immersed in $H_2O_2:H_2SO_4$ (30%:70%) for 30 minutes at room temperature and wash with Milli Q and dry under nitrogen flow.

3.4 Surface Modification

The slide was immersed in acetone solution containing 2% APTES for 2 minutes and rinsed with acetone to remove unbound silane. Then, it was washed with Milli Q and dried in an oven at 70°C for 1 hour. After that, the slide was immersed in succinic acid anhydride for 2 hours at room temperature to produce carboxyl group on the surface. The slide was rinsed with phosphate citrate buffer pH 4.6 and dried under nitrogen flow.

3.5 Antibody Immobilization

A 0.5-1 μ l of mixture solution between EDC, NHS and antibody was spotted on the surface for 1 hour at room temperature. Figure 3.1 shows a schematic diagram of our antibody-immobilized glass slide. The diameter of each spot was approximately 1.2 ± 0.1 mm with 5 mm spacing. There are 90 spots within one slide, allowing for 90 experiments. The reaction was terminated with Tris-HCl buffer 2 minutes, washed with PBS, and blocked with 1% BSA in PBS 1 hour at 37 °C before washing the last step with PBS.

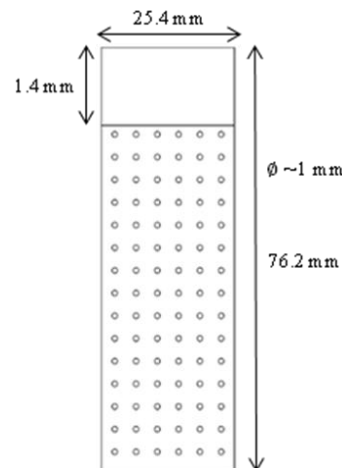


Figure 3.1 Design

3.6 Immunoassay

Samples were added to the previously spotted antibody and incubated for 1 hour at room temperature. The slide was washed with PBS before the secondary biotinylated antibody was added and incubated for 1 hour at room temperature. The washing step was repeated and the fluorescence labeled streptavidin was added to detect the signal. The signal was scanned by a fluorescent scanner (Typhoon) and the fluorescent intensity was analyzed with ImageQuant TL software.

3.7 Enzyme-Linked Immunosorbent Assay

3.7.1 NGAL

A human NGAL ELISA kit (R & D Systems, Minneapolis, MN) was used to detect human NGAL in plasma sample. Briefly, the assay diluent (100 μl /well) and samples (healthy plasma samples were diluted 100 folds and patient plasma samples were diluted 800 folds) were added (50 μl /well) to the antibody coated microwell and incubated for 2 hours at 2-8°C. The plate was washed four times. Peroxidase conjugated anti-Human NGAL antibody was subsequently added (200 μl /well) and incubated for 2 hours at 2-8°C. The washing step was repeated. A substrate solution (200 μl /well) for peroxidase (3,3',5,5'-tetramethyl benzidine and H_2O_2) was added before incubating for 30 minutes at room temperature. The reaction was stopped by addition of 1 mol/L H_2SO_4 (50 μl /well). The plate was read using a wavelength of 450 nm in a microplate reader (Tecan Group, Switzerland).

3.7.2 Interleukin-18

A human IL-18 ELISA kit (R & D Systems, Minneapolis, MN) was used to detect human IL-18 in plasma sample. Briefly, the samples (plasma samples were diluted 5 fold) were added (100 μl /well) to the antibody coated microwell and incubated for 1 hour. The plate was washed four times. Peroxidase conjugated anti-Human IL-18 antibody was subsequently added (100 μl /well) and incubated for 1 hour. The washing step was repeated. A substrate solution (100 μl /well) for peroxidase (3,3',5,5'-tetramethyl benzidine and H_2O_2) was added before incubating for 30 minutes at room temperature. The reaction was stopped by addition of 0.5 mol/L H_2SO_4 (100 μl /well). The plate was read using a wavelength of 450 nm in a microplate reader (Tecan Group, Switzerland).

CHAPTER 4 RESULTS AND DISCUSSIONS

4.1 Measurement of contact angles

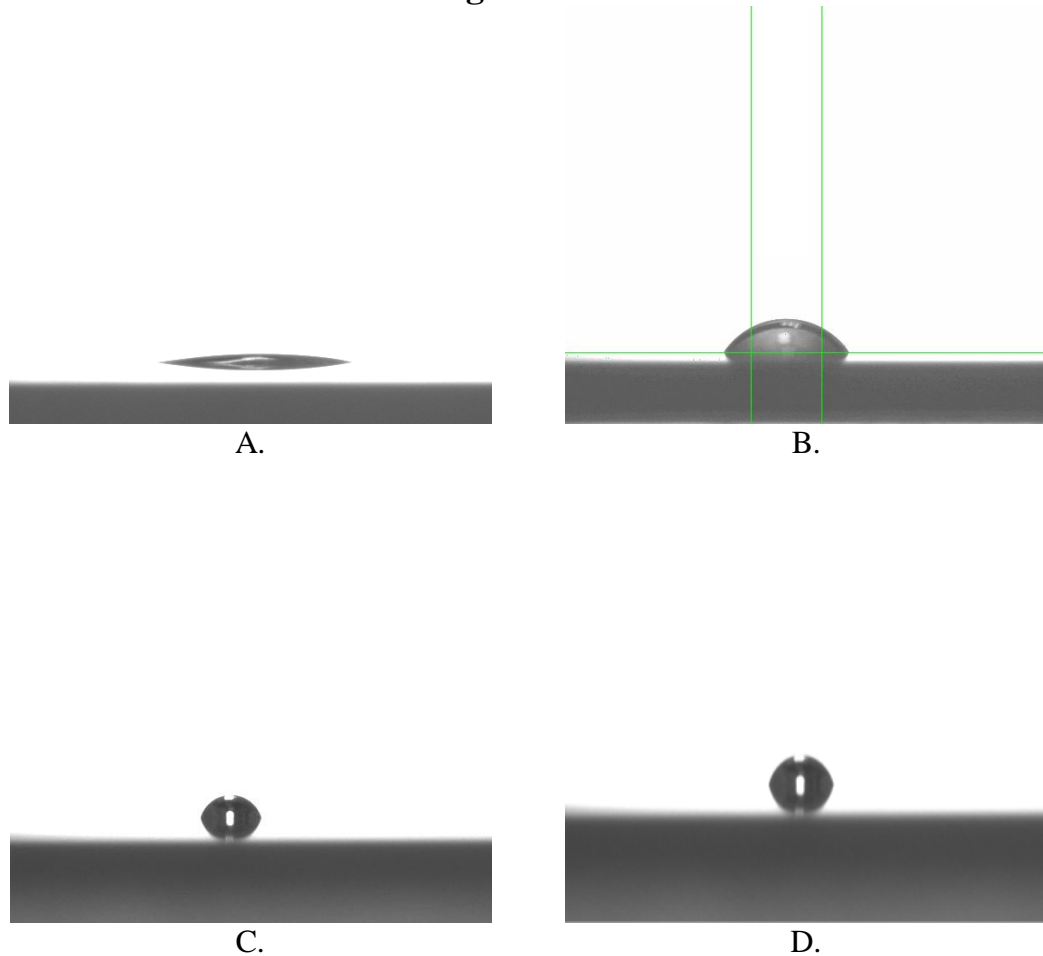


Figure 4.1 Water contact angle image
A. Piranha cleaning,
B. APTES-modified,
C. SAA-modified and
D. immobilized antibody

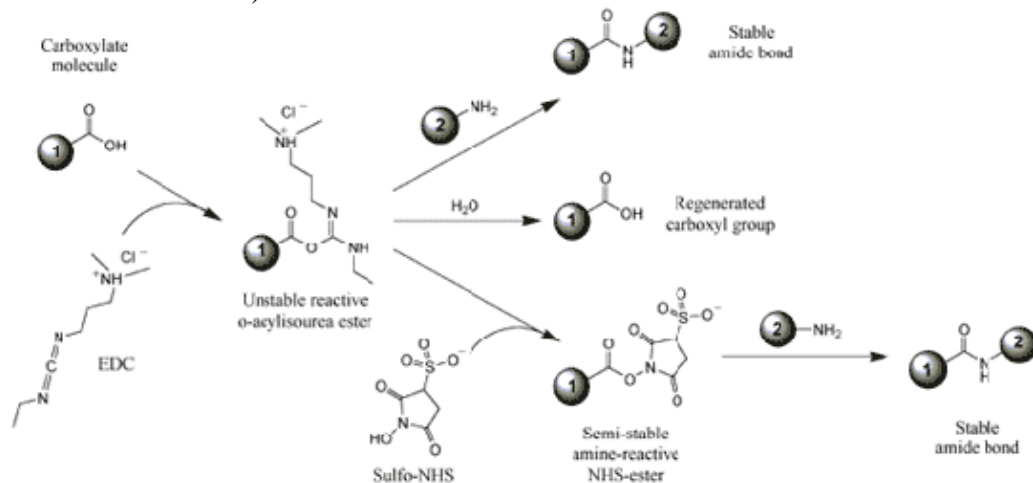
A glass slide was cleaned with 1M NaOH and Piranha's solution ($\text{H}_2\text{O}_2:\text{H}_2\text{SO}_4$) [45] before use. Then it was modified with 3-aminopropyltriethoxysilane (APTES). The cleaned glass slide was measured for its contact angle. It was 17.5° , indicating that the surface of slide was hydrophilic as shown in figure 4.1a. The contaminants on surface were removed. After the treatment with APTES, the water contact angle of the surface increased to 56.7° which means that there was the deposition of silane layer on surface. Then, the glass slide was treated with succinic acid anhydride to generate the carboxyl group. The contact angle decreased from 56.7° to 49.6° . The surface became more hydrophilic due to carboxyl group. The surface contact angle increased to 75° after the immobilization of antibody via the reaction between carboxyl group from slide's surface and the amino group of the antibody. This result shows that antibody was successfully immobilized onto the glass slide.

Table4.1 Water contact angles of Piranha cleaning, modified - and immobilized antibody glass surfaces

Sample Type	Piranha cleaning	APTES-modified	SAA-modified	Immobilized
WCA	17.5°	56.7°	49.6°	75°

4.2 Surface Modification & Antibody Immobilization

There are many methods to immobilize antibody on glass surface. This study uses heterobifunctional cross linkers, Carbodiimide hydrochloride (EDC) and N-hydroxysuccinimide (NHS), to covalently immobilize capture antibody (Normal rabbit IgG as a model and Alexa flour 488 goat anti-rabbit as a secondary antibody were purchased from Invitrogen, Canada) The immobilization mechanism is based on covalent bonding between the amino groups of the antibody and carboxyl-terminated surface of the modified glass slide as shown in Figure4.2. The experiment shows comparative the efficiency of immobilization by using only EDC and EDC with NHS (Table4.2 and Table4.3).

**Figure4.2** Structures of EDC and NHS**Table4.2** The concentration of the solution between EDC and antibody

	Negative control	1	2
EDC($\mu\text{g/ml}$)	20	20	20
Antibody($\mu\text{g/ml}$)	-	10	100

Table4.3The concentration of the solution between EDC, NHS and antibody

	Negative control	1	2
EDC($\mu\text{g/ml}$)	20	20	20
NHS($\mu\text{g/ml}$)	30	30	30
Antibody($\mu\text{g/ml}$)	-	10	100

The result shows that antibody concentration at 100 $\mu\text{g/ml}$ has high fluorescence intensity. The intensity is proportional to the antibody concentration, as high concentration of antibody gives high fluorescent intensity. Using the EDC+NHS linker gives more efficiency than an EDC linker. The addition of NHS stabilizes the amine-reactive intermediate by converting it to an amine-reactive NHS ester, thus increasing the efficiency of EDC-mediated coupling reactions as shown in Figure4.3. Thus, the optimized condition for antibody immobilization is the mixture between antibody, EDC 20 $\mu\text{g/ml}$ and NHS 30 $\mu\text{g/ml}$.

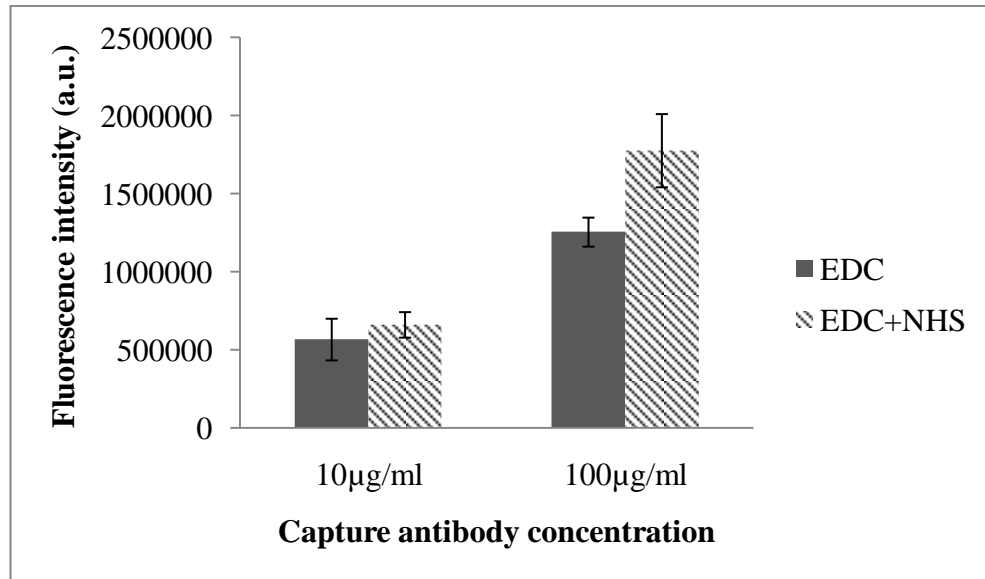


Figure4.3 Bar plots between rabbit IgG concentration and fluorescence intensity

4.3 The efficiency of the concentration of linkers to immobilize the antibody

This study compares the concentration of linkers to immobilize antibody. The concentration of the mixed solution shows in Table4.4.

Table4.4 The concentration of the solution between EDC, NHS and antibody

	1	2	3	4
EDC(mM)	0.1	0.1	2	2
NHS(mM)	0.25	0.25	5	5
Antibody(µg/ml)	10	100	10	100

The result shows that using higher concentration of linkers (EDC 0.2mM and NHS 0.5mM) for antibody immobilization gives more efficiency in both antibody concentration at 10 and 100µg/ml as shown in Figure4.4. However, higher concentration of linkers may not increase the efficiency of immobilization due to excess the molar ratio of EDC/NHS to antibody. The optimal crosslinker-to-antibody molar ratios are necessary to be determined.

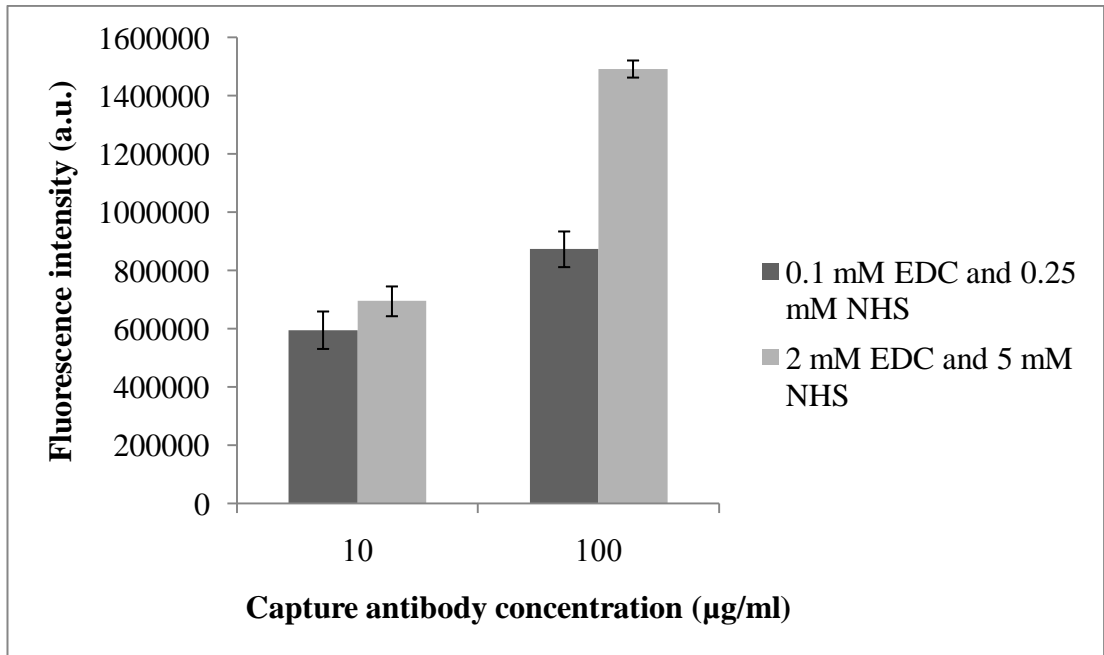


Figure4.4 Bar plot between fluorescence intensity and antibody concentration

4.4 Neutrophil gelatinase-associated lipocalin (NGAL)

4.4.1 Optimized capture anti-NGAL antibody

The anti-NGAL antibody was immobilized on surface at various concentrations (2, 5 and 8 µg/ml, according to manufacturer's instruction; R&D system, USA) to determine an optimized capture concentration to perform an immunoassay to get the highest signal and the lowest background. The result showed that the anti-NGAL antibody concentration at 8 µg/ml give the highest fluorescence intensity as shown in Figure4.5. Thus, 8 µg/mL of capture antibody was used for further studies

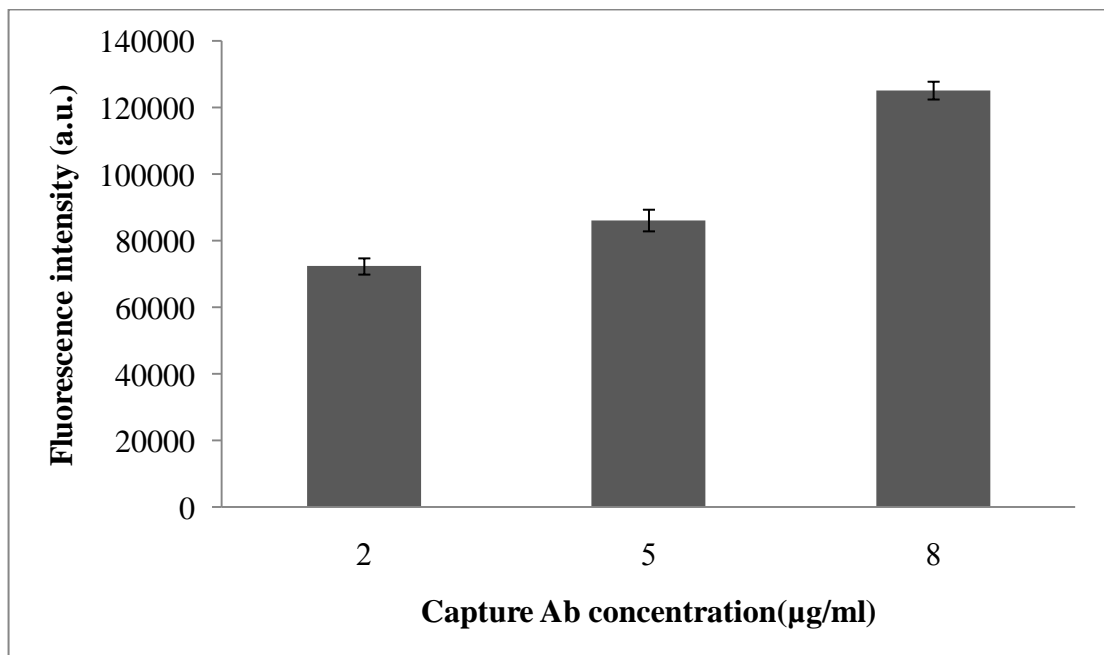


Figure4.5 Optimized capture anti-NGAL antibody

4.4.2 Calibration curve NGAL

The recombinant NGAL was diluted between 10-1000 ng/ml. Each concentration was repeated 6 times. Figure4.6A. shows the location of each concentration of NGAL. “neg.” represents a negative control which means the spots that were immobilized with antibody but the sample contained no protein to determine the noise of the system.. “blank” represents the location which there was no immobilized antibody to determine background. The result shows that the concentration of recombinant NGAL at 1000 ng/ml gives the maximum fluorescence intensity. The fluorescence intensity of a negative control or the concentration of protein at 0 ng/ml is lowest. The intensity of fluorescence is proportional to the protein concentration. There was no nonspecific binding outside the immobilized antibody location. Figure4.6B shows the fluorescence image of the slide. The diameter of each slide was measured with ImageJ software which is 1.2 ± 0.1 mm.

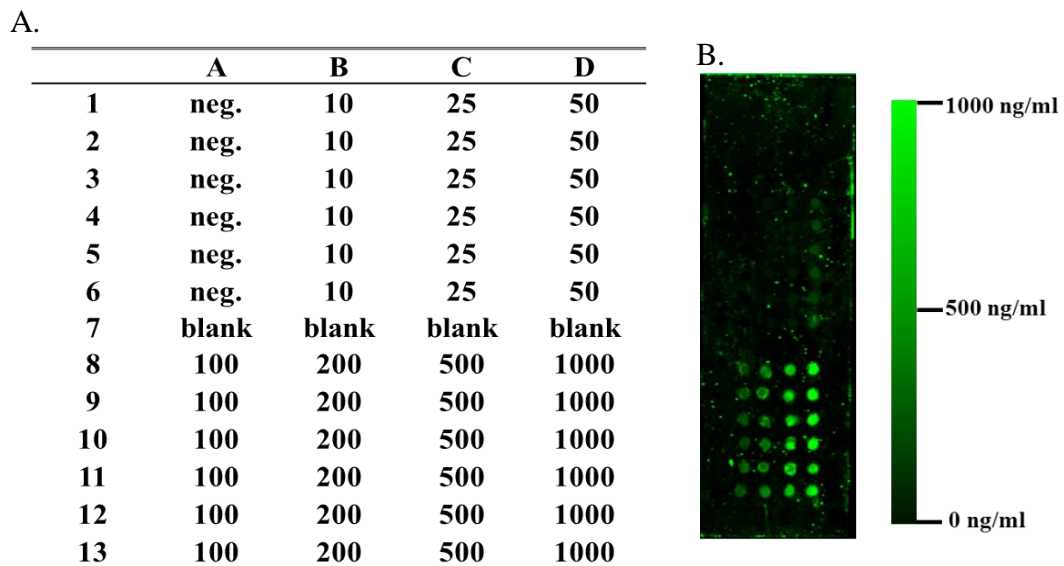


Figure4.6 A. The location of each concentration of NGAL
B. Fluorescence image

The fluorescence intensity of each spot was analyzed with Imagequant tl and calculated by subtracting the intensity obtained from the negative control to generate calibration curve. The fluorescence intensity is linearly proportional to the NGAL concentration between 50 to 1000 ng/ml as shown in Figure4.7. The correlation coefficient (R^2) is 0.9903, which is considered to be quite high.

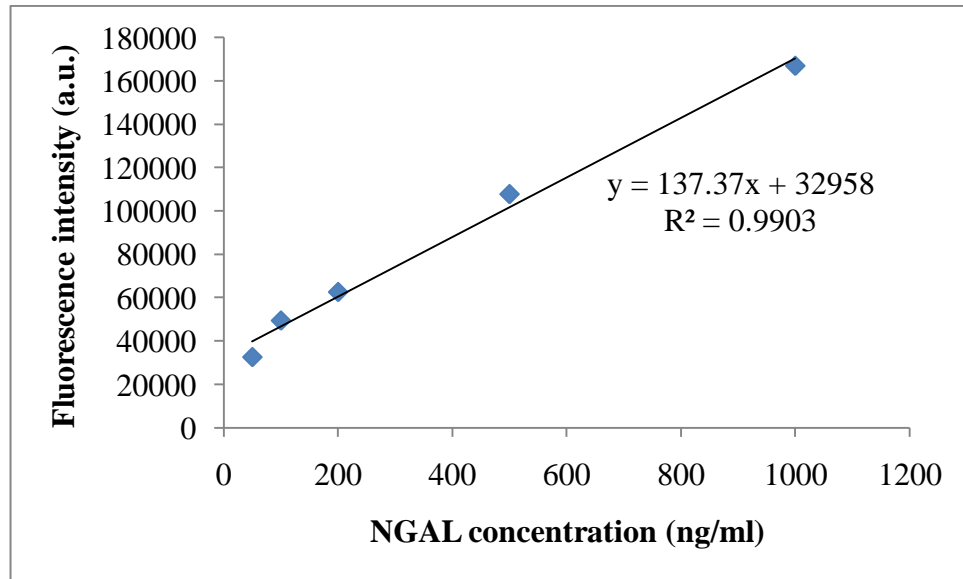


Figure4.7 Calibration curve of NGAL

4.4.3 Reliability assay

The precision or reproducibility of assay can be shown in coefficient of variable (CV), Intra-assay CV and Inter-assay CV. The CV can be calculated as shown in Eq.4.1 which calculates from concentration of protein [46].

$$\%CV = \frac{\text{Standard deviation}}{\text{Mean}} \times 100 \quad (4.5.3.1)$$

The measurement of three known concentrations of recombinant NGAL 250, 500 and 1000 ng/ml were repeated twenty times on one slide to test the intra-assay precision. Twenty replicates of each sample in five separate assays were used to test the inter-assay precision. The error of the measured concentrations from the actual concentrations calculated using the equation Eq.4.2

$$\%Error = \frac{|\text{measured conc.} - \text{actual conc.}|}{\text{actual conc.}} \times 100 \quad (4.5.3.2)$$

The intra-assay is used to determine the spot-to-spot variability. As shown in Table4.5 the intra-assay CV was ranged from 4.54% to 1.83% and the average of intra-assay CV was 2.67%. The inter-assay shows the slide-to-slide reproducibility. The inter-assay CV of this system was ranged from 1.67% to 1.06% and the average was 1.28%. According the research of biological studies [47], the intra-assay CV of less than 10% is generally acceptable and the inter-assay CV should be less than 15%. Thus, the CVs of the intra-, and the inter-assay of this technique indicate reliable detection. Furthermore, the percentage error of measurement is less than 10, which is considered acceptable.

Table4.5 Intra- and Inter-assay of NGAL

Sample	Intra-assay			Inter -assay		
	1	2	3	1	2	3
Actual conc.	250	500	1000	250	500	1000
n	20	20	20	20	20	20
Mean(ng/ml)	264.24	508.10	950.99	263.30	508.16	952.56
%CV	4.54	1.83	1.64	1.11	1.67	1.06
%error	5.69	1.62	4.90	5.32	1.63	4.74

4.4.4 Comparison between ELISA and slide

The ELISA technique is a convention method which is high precision and accuracy. Therefore, the performance of the glass slide system was compared with that of ELISA in the term of assay time, volume of reagents consumption, sensitivity or limit of detection and the correlation coefficient (R^2) as shown in Table4.6. The reagent consumption of the slide system is less than ELISA for 200 folds. The R^2 of the ELISA (0.9922) technique is higher than the glass slide system (0.9903). Although the limit of detection is higher than Elisa method but the concentration of NGAL in plasma sample is well above the limit. Thus, the glass slide system can be applied to diagnose the patient with AKI.

Table4.6 Comparison between ELISA and glass slide of NGAL

	ELISA	SLIDE
Time	4½ hours	2½ hours
Volume of reagents	100 µl/sample	0.5 µl/sample
Limit of detection (LOD)	0.0012 ng/ml	<25ng/ml
Correlation coefficient(R^2)	0.9922	0.9903

4.5 Interleukin-18 (IL-18)

4.5.1 Optimized capture anti-IL-18 antibody

The antibody specific to recombinant human IL-18 was immobilized on a surface-treated glass slide at various concentrations of 2, 5 and 10 µg/ml (according to manufacturer's instruction; R&D system, USA) to determine the optimized concentration of the antibody for an immunoassay. The immobilization mechanism is based on covalent bonding between the amino groups of the antibody and carboxyl-terminated surface of the modified glass slide. The maximum fluorescence intensity was observed when 5 µg/ml of anti-IL-18 antibody was used for the antibody immobilization. The fluorescence intensity at 10 µg/ml was lower than that of 5 µg/ml because the steric hindrance near the immobilized antibody affected the antigen binding sites leading to a decreased antibody activity [34]. Therefore, 5 µg/mL of capture antibody was used for further studies.

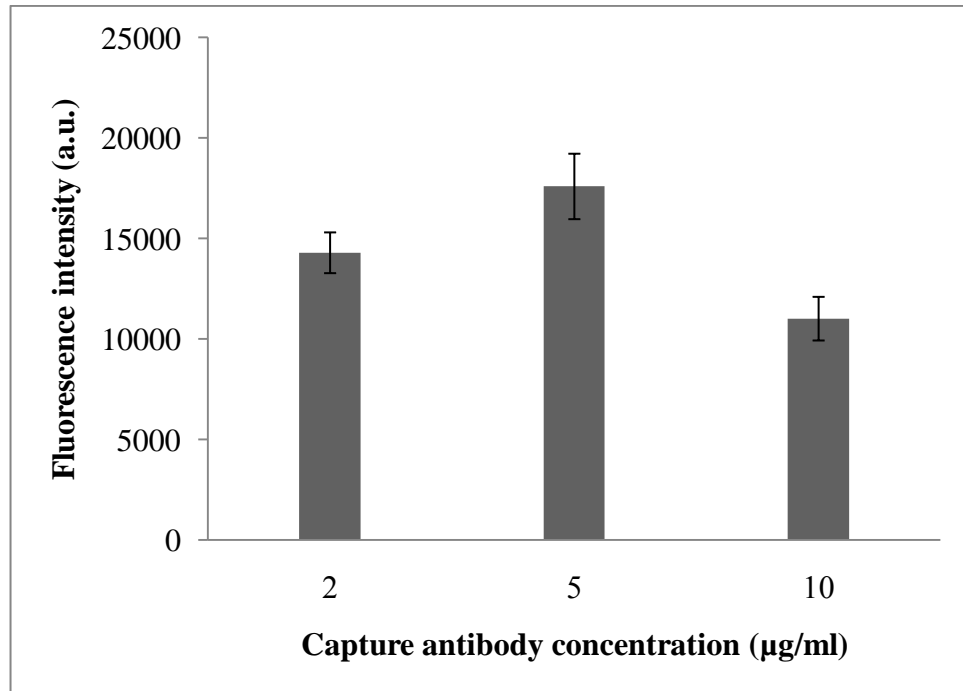


Figure4.8 Fluorescence intensities when the concentrations of immobilized antibody specific for IL-18 were 2, 5, and 10 µg/mL

4.5.2 Calibration curve

Samples containing recombinant human IL-18 were diluted in PBS at a range of concentrations between 10 to 1,000 pg/ml. The measurement of each concentration was carried out in 6 replicates. The immunoassay experiment was designed as shown in Figure 4.10(a). Blank indicates spots where there was no capture antibody immobilized to determine the noise level, while neg. represents the spots where samples containing no antigen were incubated with immobilized antibody to determine the background signal. Figure 2a shows a schematic diagram of our antibody-immobilized glass slide. The diameter of each spot was approximately 1.2 ± 0.1 mm with 5 mm spacing. There are 90 spots within one slide, allowing for 90 experiments including blank, negative and positive controls. A representative fluorescent image of the immunoassay glass slide is shown in Figure 4.10(b). The fluorescent labeled antibodies were clearly binding to the targets on the glass slide. Nonspecific binding outside the immobilized antibody spots were not observed. The background signal calculated from the negative control spots were below a detectable level. As expected, higher concentrations of the analyte resulted in higher fluorescent intensity.

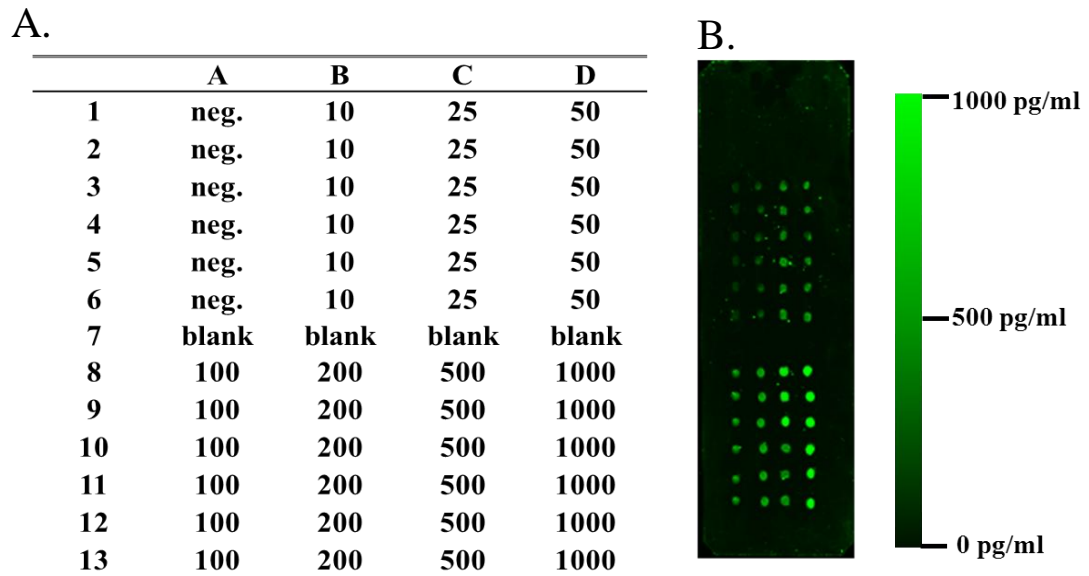


Figure4.9 A. The location of each concentration of IL-18
B. Fluorescence image

The intensity of each concentration of il-18 was calculated by subtract the negative control and plotted to generate the calibration curve (Figure4.10). The fluorescent intensity is linearly proportional to the between 25 to 1000 pg/ml in the test sample. The correlation coefficient or R^2 of this model is 0.989, which is quite high. The sensitivity or the lower detection limit (LOD) calculated based on the signal to noise ratio of 3 is 15 pg/ml.

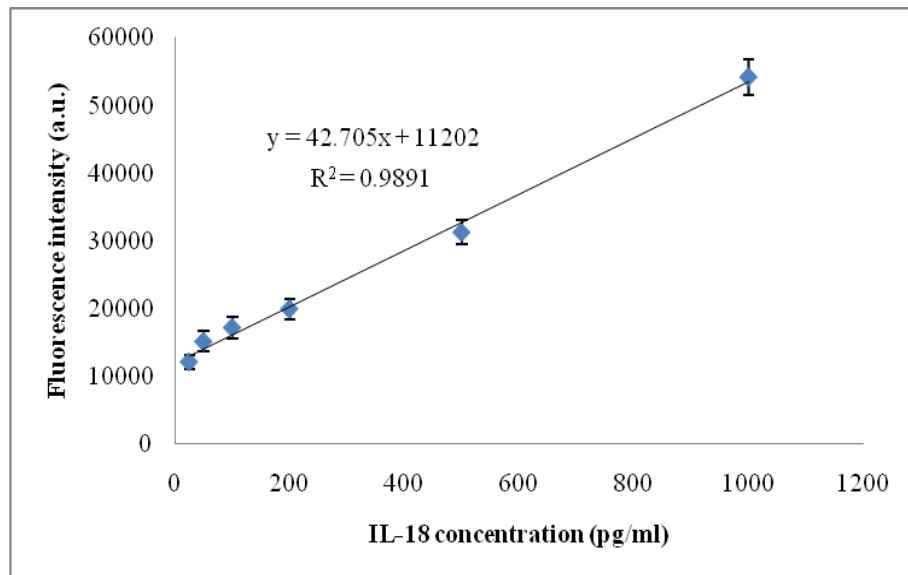


Figure4.10 Calibration curve of IL-18

4.5.3 Reliability assay

The precision or reproducibility of assay can show in Intra-assay CV and Inter-assay CV. The CV and the percentage error measurement can be calculated as show in Eq4.1 and Eq.4.2 as mentioned in above paragraph. Three known concentrations of recombinant IL-18 50, 100 and 200 pg/ml were replicated twenty times on one slide to test the intra-assay precision.

Twenty replicates of each sample in five separate assays were used to test the inter-assay precision. According to Table4.7, The intra- assay of this method is below 10% and the inter-assay is well-below 15%. Thus, the CVs of the intra-, and the inter-assay of this technique indicate reliable detection. Moreover, the % error of this measurement is less than 10, which is considered acceptable. As a result, this immunoassay system can be used to accurately analyze the recombinant human IL-18.

Table4.7 Intra- and Inter-assay of IL-18

Sample	Intra-assay			Inter -assay		
	1	2	3	1	2	3
Actual conc.	50	100	200	50	100	200
n	20	20	20	20	20	20
Mean(ng/ml)	54.23	98.50	198.74	53.48	104.63	202.03
%CV	7.77	9.03	2.45	2.81	4.96	1.32
%error	8.46	1.50	0.63	6.96	4.63	1.02

4.5.4 Comparison between ELISA and slide

Various concentrations of recombinant human IL-18 were analyzed with an ELISA kit and compared with those measured from the glass slide system. The calibration curve generated from immunoassays using ELISA was compared with that of the glass slide system at the same concentrations. According to Table4.8, the R^2 of the ELISA method (0.9982) is better than that of the glass slide system (0.9891). The sensitivity of ELISA is 12.5 pg/ml as shown in the manufacture's instruction whereas that of glass slide is 15 pg/ml. The slight difference in the limit of detection indicates that this glass-slide system is quite sensitive.

Table4.8 Comparison between ELISA and glass slide of IL-18

	ELISA	SLIDE
Volume of reagents	100 µl/sample	0.5 µl/sample
Limit of detection (LOD)	12.5 pg/ml	15 pg/ml
Correlation coefficient(R^2)	0.9982	0.9891

4.6 Cross-reactivity

The multiplexing immunoassay technique is capable of detecting more than one antigen at the same time within one glass slide. Therefore, cross-reactivity is more concern to reduce non-specific binding and the error from competitive binding between analytes. To examine cross-reactivity of the antibody set employed in this study, three known concentrations of IL-18 (100, 200 and 1000 pg/ml) and NGAL (250, 500 and 1000

ng/ml) were spotted on the location of non-specific antibody. The positive control was the location which the samples (a mixture of 1000 pg/ml of IL-18 and 1000 ng/ml NGAL) were spotted on the specific antibody. As shown Figure4.11, the anti-human IL-18 antibody pair was specific for the recombinant human IL-18, but not for recombinant human NGAL. In the same way, the anti-human NGAL antibody pair was specific for the recombinant human NGAL. Both of the antibodies recognize their specific antigen. Therefore, this antibody set is suitable for a multiplexing immunoassay.

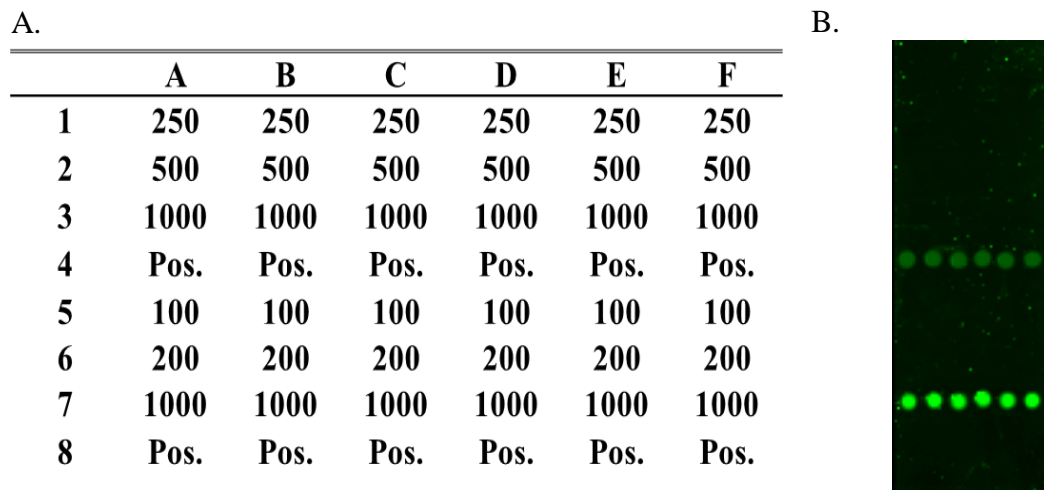


Figure4.11 Cross reactivity experiment

A. row 1-4 where anti-IL-18 antibody was immobilized, the protein NGAL was added at row 1-3 and row 5-8 where anti-NGAL antibody was immobilized, the protein IL-18 was added at row 5-7, Pos. was positive control

B. The fluorescence image

4.7 Analysis of plasma samples

The samples were analyzed in parallel with standard protein dilution series to allow for quantification of the samples. The measurement of each plasma sample was repeated three times and the measurement of the standard protein was repeated twice on one slide. According to Table4.9, the average plasma NGAL concentration in healthy control was 51.20 ± 10.07 ng/ml (mean \pm SD) and in AKI was 353.14 ± 153.01 ng/ml. The average level of plasma IL-18 in the control samples was 265.95 ± 135.09 pg/ml and in the AKI samples was 1475.93 ± 1163.27 pg/ml. As expected, the concentration of two biomarkers in plasma sample of patients with AKI was much higher than those of the healthy controls.

Table4.9 Plasma NGAL (ng/ml) and IL-18 (pg/ml) obtained by glass slide system

	Healthy control	AKI
n	20	20
NGAL (ng/ml)	51.20 ± 10.07 (30.80-73.94)	353.14 ± 153.01 (123.26-702.27)
IL-18 (pg/ml)	265.95 ± 135.09 (106.86-664.37)	1475.93 ± 1163.27 (141.75-4886.01)

4.8 Comparison between glass slide system and ELISA

The planar platform of immunoassay in this study for the measurement of AKI biomarkers (NGAL and IL-18) has been developed based on the same principle as ELISA. In order to check the reliability of the glass slide system, the measurement of

two proteins from slide was compared with the value from ELISA method (Table4.10). The result was shown in scatter plot between the measurement from ELISA and from the glass slide (Figure4.12 and Figure4.13). The correlation of two methods is linear relationship. The measured value between slide system and ELISA are not significant different ($p>0.05$). Both method give similar measurement.

Table4.10 The levels of NGAL and IL-18 obtained by glass slide and ELISA

Sample	NGAL (ng/ml)		IL-18 (pg/ml)	
	Slide	ELISA	Slide	ELISA
H1	49.94	55.94	339.22	344.58
H2	50.85	53.98	295.82	309.58
H3	42.87	47.53	499.64	491.04
H4	57.50	63.26	653.69	684.17
H5	50.72	58.23	290.91	273.54
H6	55.56	63.51	138.34	180.21
H7	64.94	70.83	264.46	247.08
H8	32.29	35.14	133.03	157.29
H9	61.98	68.71	106.87	137.71
H10	33.78	38.51	182.48	182.08
H11	58.09	65.62	213.60	202.92
H12	49.61	55.64	215.54	219.58
H13	48.67	50.19	315.62	301.46
H14	49.15	56.21	206.81	210.00
H15	51.29	55.73	173.54	197.50
H16	47.18	50.84	292.65	270.00
H17	34.46	45.61	100.39	119.38
H18	77.33	79.61	321.98	337.08
H19	54.66	65.56	209.62	206.88
H20	66.51	66.52	361.22	356.46
2	244.73	245.25	1445.13	1612.71
3	374.50	376.63	1373.60	1363.54
B12	267.58	287.28	1799.72	1772.50
B13	118.26	135.39	245.44	273.13
B15	346.24	367.19	429.69	432.92
B23	233.57	238.38	1335.82	1408.75
B24	286.20	293.56	582.02	573.75
B27	452.80	467.10	537.10	509.17
B28	264.89	262.93	136.14	134.17
B29	599.31	606.99	2810.66	3015.62
B30	244.89	249.36	761.80	763.75
B31	240.00	229.91	625.96	654.17
B32	552.89	604.69	1810.59	1841.88
B33	697.37	697.50	1685.67	1795.00
B34	216.86	217.56	3389.71	3420.21
B35	367.92	362.81	2243.46	2271.46
B37	568.20	567.23	2267.28	2505.42
B40	256.01	263.32	455.50	467.92

B41	278.50	283.66	4900.74	4962.71
B43	386.27	382.65	1572.26	1704.17

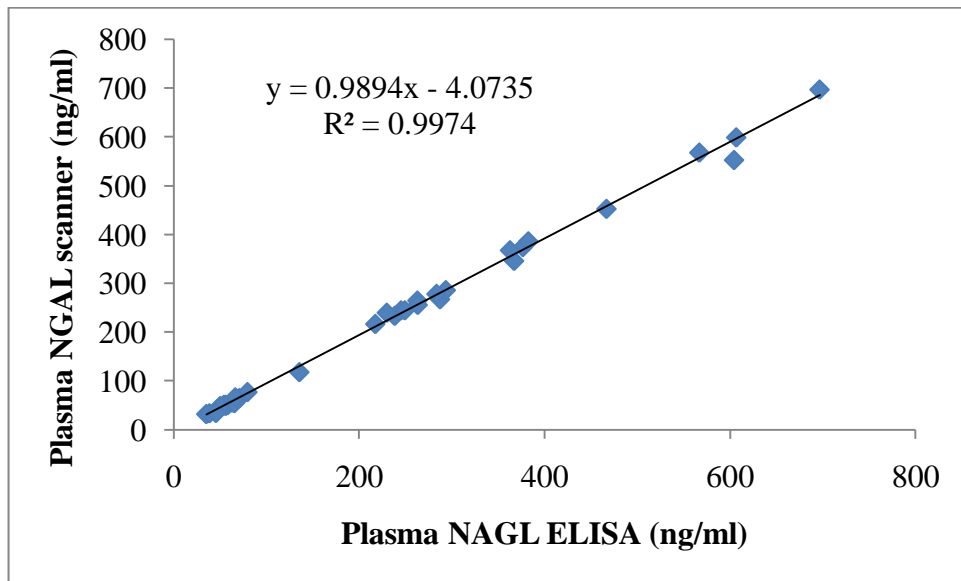


Figure4.12 Scatter plots showing the linear relationship between the gold standard ELISAs and the fluorescence scanner of NGAL

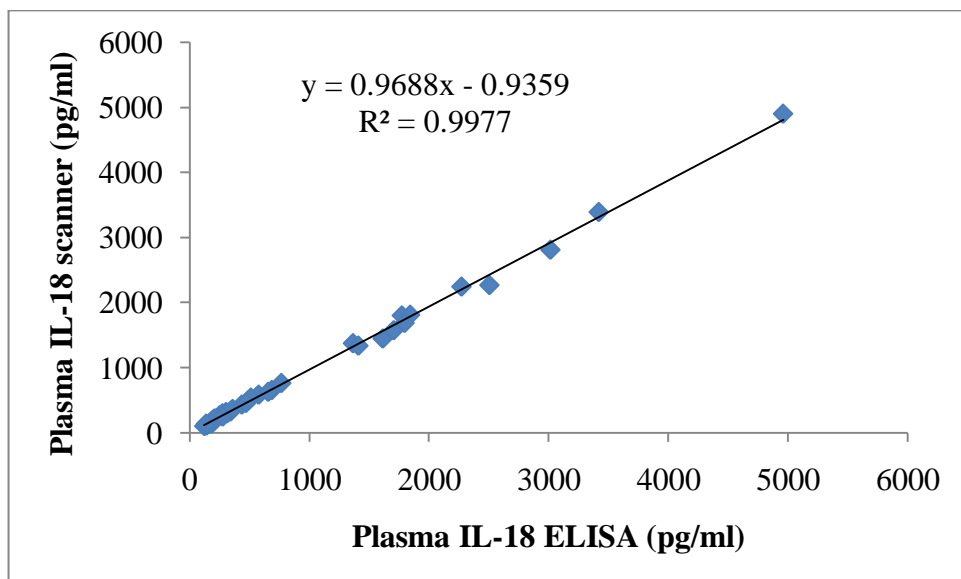


Figure4.13 Scatter plots showing the linear relationship between the gold standard ELISAs and the fluorescence scanner of IL-18

According to Figure 4.13 and 4.14, the measurement of both NGAL and IL-18 proteins from the glass slide system matched well with those from ELISA. Both data sets were highly correlated. The slopes of both regression lines are close to 1, indicating that the deviation between the values measured by ELISA and by our system was insignificant. This result shows that the glass slide system has been validated and that it is possible to use this system in place of ELISA for the detection of NGAL and IL-18.

4.9 Preservation of the immobilized antibody activity

The longer array lifetime will make this platform possible for commercialization. The immobilized slides were dried and stored under different conditions (Table4.11) to study the effect of temperature, humidity and oxygen on immobilized antibody for 1 day, 1 week, 2 weeks and 4 weeks. After that, they were operated as described previously. Only in condition 4, the slide was purged with nitrogen to completely remove oxygen. Three known concentrations of the recombinant human NGAL (250, 500, and 1000 ng/ml) and IL-18 (50, 100 and 200 pg/ml) were used to study the stability of the printed slides.

Table4.11 The condition for keeping immobilized slide

	Temperature	Moisture	Oxygen transfer
1	Room temperature	yes	yes
2	4°C	yes	yes
3	4°C	no	yes
4	4°C	no	no

4.9.1 The effect of temperature to immobilized slide

According to Figure 4.14 to Figure 4.15, temperature strongly affected the quality of the immobilized antibody on the glass slide. The fluorescence intensity of the immobilized slide which was stored at room temperature was significantly less than that of the slide stored at 4°C in every concentration of both proteins. An increase in temperature induces the change in an antibody structure and conformation, leading to reduction of immunologic activities of antibody [48,49]. Therefore, the lower temperature was chosen as one of the storage conditions for further study.

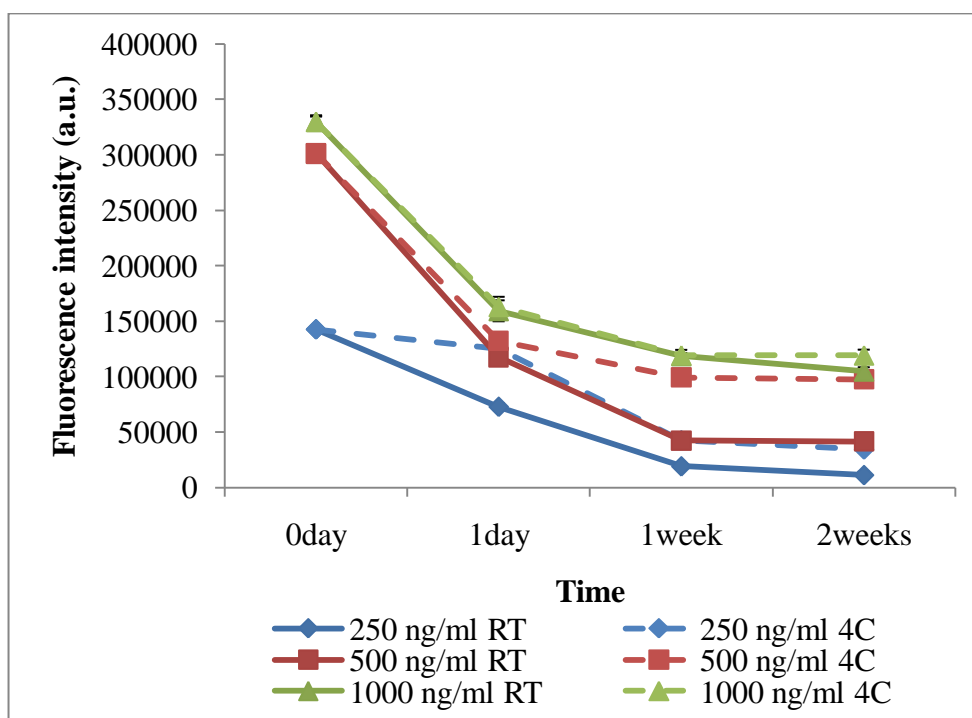


Figure4.14 The effect of temperature on the stability of immobilized anti-human NGAL antibody slide at room temperature (RT) and 4°C in various NGAL concentrations

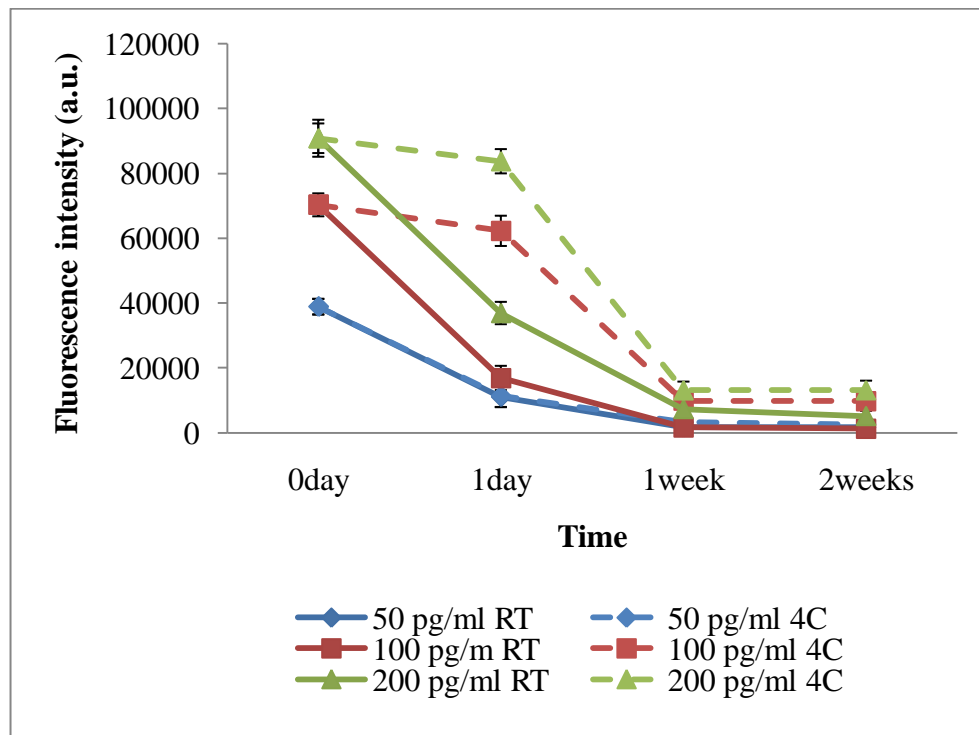


Figure 4.15 The stability of immobilized anti-human IL-18 antibody slide at room temperature (RT) and 4°C in various IL-18 concentrations

4.9.2 The effect of humidity to immobilized slide

In this study, the effect of moisture on the activity of the immobilized slides was evaluated. Silica gel was used to remove moisture from the storage container. In Figure 4.16 and Figure 4.17, the slides that were stored in humid environment resulted in less fluorescence intensity than the slides were kept without humidity. The fluorescence intensities in all concentrations of NGAL and IL-18 were maintained up to 1 week when the slides were stored without humidity, while the activities of the immobilized anti-NGAL and anti-IL-18 antibodies significantly dropped after 1 day when stored under normal condition. This may be caused by the moisture sensitivity of the linkers, EDC and NHS [33]. It is possible that the moisture weakens the bond between the linkers and the glass slide, causing the detachment of the linker during multiple washing steps. As a result, less number of capture antibody was present on the glass slide, leading to lower fluorescence signal. Moreover, the previous study demonstrated that the antibody stored in a desiccator did not show any loss in its activity [50,51].

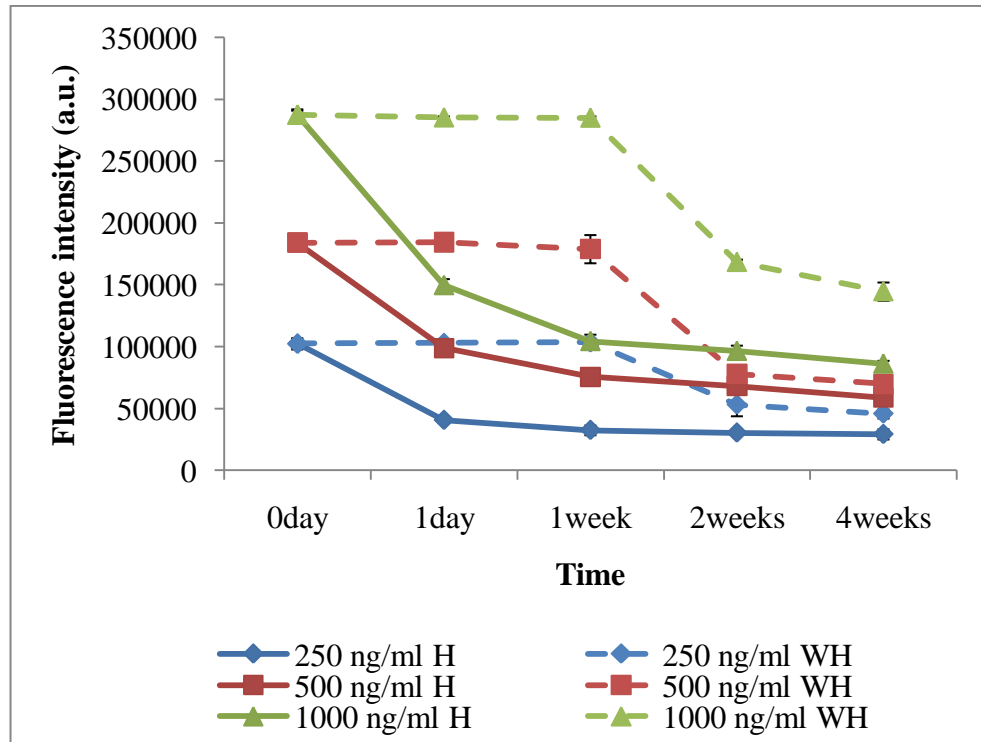


Figure4. 16 The effect of humidity on stability immobilized anti-human NGAL antibody slide with and without humidity (H, WH) in various NGAL concentrations

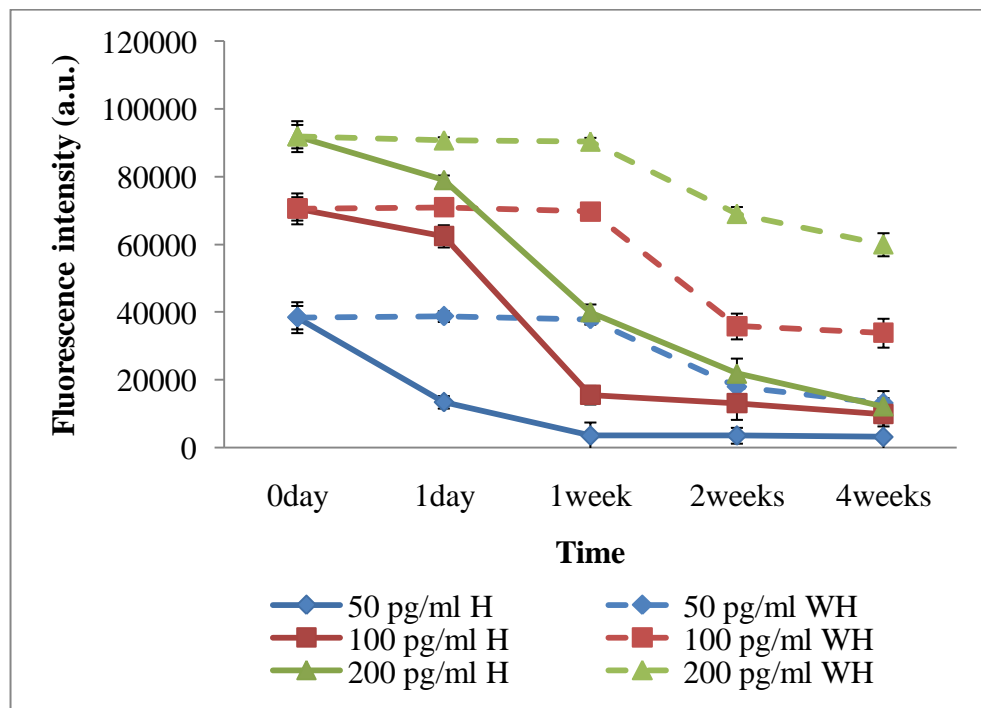


Figure4.17 The effect of humidity on stability immobilized anti-human IL-18 antibody slide with and without humidity (H, WH) in various IL-18 concentrations

4.9.3 The effect of oxygen to immobilized slide

It is possible that the antibody can be oxidized resulting in the denaturation of the protein and loss activity. As a result, the effect of oxygen on the prolonged activity of antibody was studied. The condition without oxygen can be accomplished by purging the storage container with nitrogen gas. Our results show that the fluorescence intensities were initially constant, but gradually decrease after 1 week in storage in both conditions. Interestingly, the signal intensity obtained from the printed slide without nitrogen purge was decreased more in comparison to the nitrogen storage. Therefore, we believe that oxygen affects the printed slide (Figure4.18). The immobilized antibody was oxidized with oxygen, leading to denaturation and decrease activity of antibody [52]. In addition, the conformation of antibody changes because the oxidation of amino acid in antibody leads to the degradation of antibody [53]. For the anti-IL18 printed slides, the fluorescence intensities of two studies were similar (Figure4.19). The intensities of the non-treated and treated slides were initially constant and decreased after 1 week. Hence, we believe that oxygen affects the antibody's activities when stored longer than 1 week.

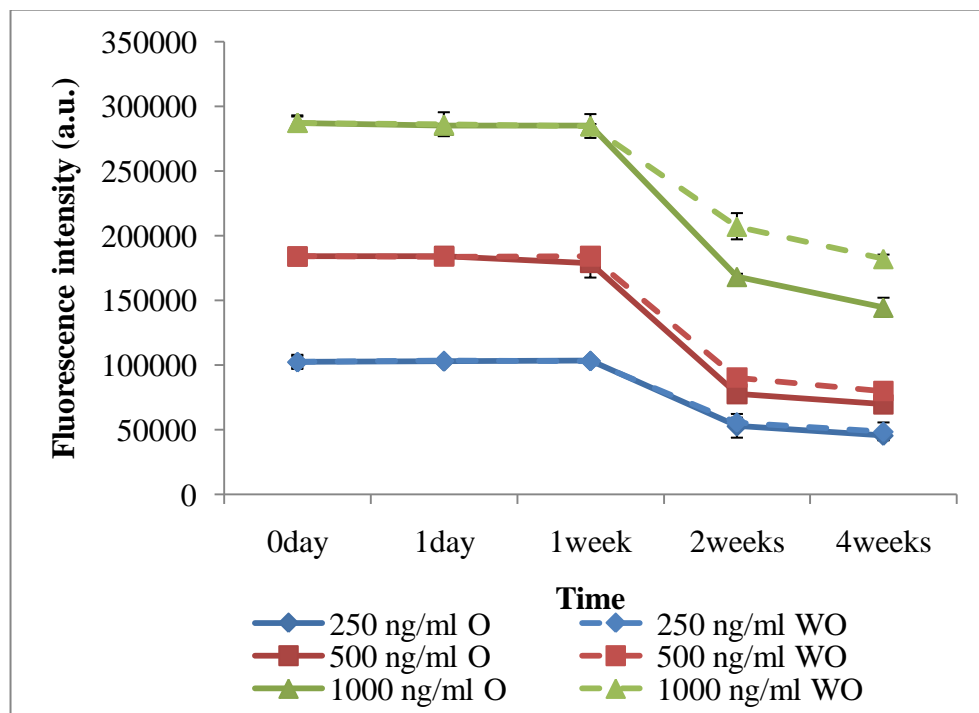


Figure4.18 The effect of oxygen on stability immobilized anti-human NGAL antibody slide with and without oxygen (O, WO) in various NGAL concentrations

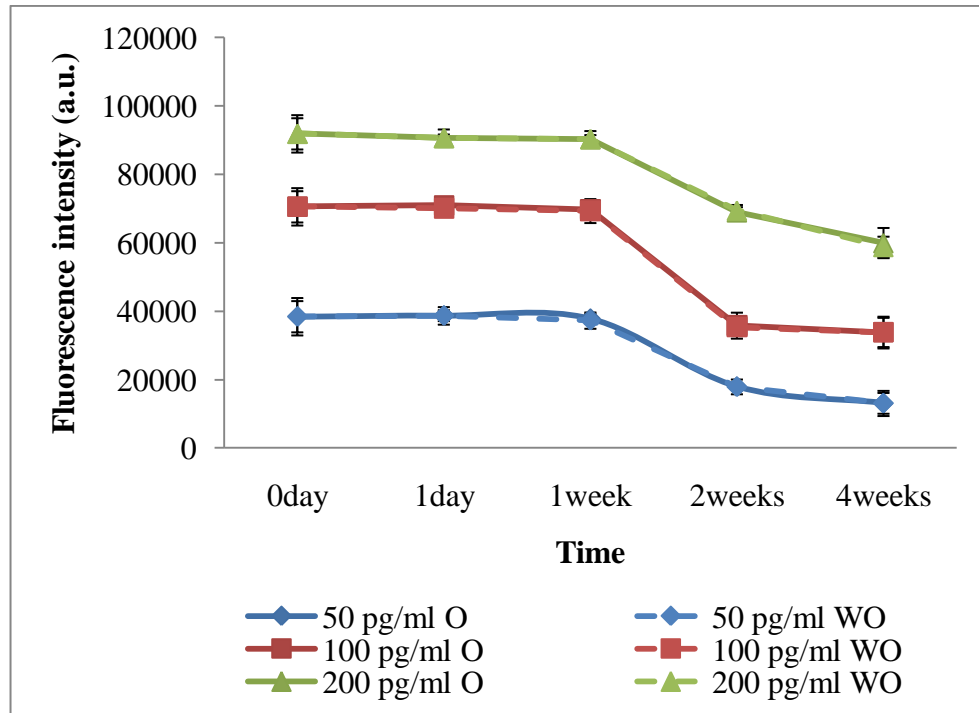


Figure4. 19 The effect of oxygen on stability of immobilized anti-human IL-18 antibody slide with and without oxygen (O, WO) in various IL-18 concentrations

High temperature, humidity and oxygen affected the immobilized slides. The results demonstrated that the printed slide could be stored following condition 4 which is 4°C, no humidity and oxygen environment and should be used within one week. The most important concern is photo bleach; therefore, the storage bag should provide light protection capability, such as an aluminium foil bag [50,51].

4.10 Influence of incubation time on signal intensity

The shorter assay time can help save time and get results quickly to diagnose AKI for early therapy to prevent kidney failure. This study reduces the incubation time in each step as shown in Table4.12. In condition 3 to 6, the biotinylated antibody was mixed with labeled streptavidin to reduce the numbers of processing steps.

Table4.12 The incubation time of each step

	Sample	Biotinylated antibody	Labeled streptavidin	Biotinylated antibody/ Labeled streptavidin	Total time
1	1 hour	1 hour	½ hour	-	2½ hours
2	1 hour	½ hour	½ hour	-	2 hours
3	1 hour	-	-	1 hour	2 hours
4	1 hour	-	-	½ hour	1½ hours
5	½ hour	-	-	1 hour	1½ hours
6	½ hour	-	-	½ hour	1 hour

The concentration of protein NGAL and IL-18 was diluted at the same concentration (50 to 1000 ng/ml of NGAL and 25 to 1000 pg/ml of IL-18) to generate a calibration curve to study the assay time. According to Figure4.20, the assay time in each step was reduced to detect NGAL. The result shows that the standard incubation (condition 1) time gave the highest fluorescence intensity. The lowest intensity was observed in condition 2, which the incubation time of biotinylated antibody and labeled streptavidin was reduced separately. It is possible that half an hour incubation is not sufficient for the protein to conjugate with the antibody. In condition 3 to condition 6, the fluorescence intensities were similar, showing that mixing biotinylated antibody with labeled streptavidin did not affect the immunoassay performance. According to our results, the incubation time directly affects on the reaction between proteins or the fluorescence intensity. However, a linear relationship between the protein concentrations and the fluorescence intensities can be observed in every condition. The slope of calibration curve in each condition was similar. Therefore, the reduction in incubation time is considered acceptable in practice.

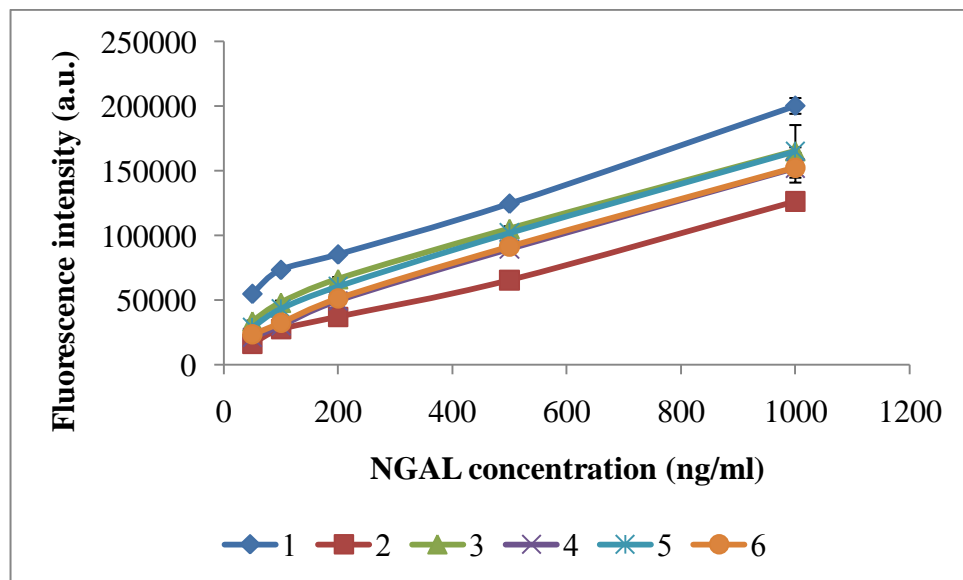


Figure4.20 The effect of incubation time to assay in NGAL protein

Figure4.21 shows the calibration curves in each condition to study shorter assay time for IL-18 detection. The highest fluorescence intensity was observed in condition 1 which was the standard time. The shortest total assay time (condition 6) gave the lowest intensity, which reduced 35% of the intensity of the standard time. Nevertheless, the calibration curve in every condition shows a linear relationship and the slope in each condition was alike.

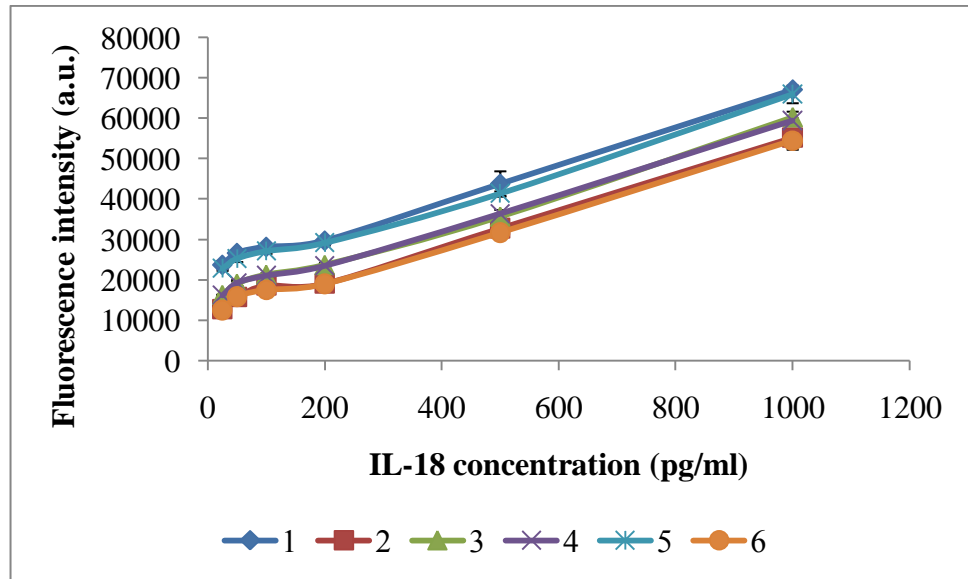


Figure4.21 The effect of incubation time to assay in IL-18 protein

The results of both tests indicated that the immunoassay performance was not affected by the shorter assay time. Thus, reducing incubation time can still be used to detect the NGAL and IL-18 to diagnose AKI. However, the standard assay time give the highest fluorescence intensity. If speed is required to diagnose AKI for early therapy to prevent kidney failure, the condition 6 is acceptable.

CHAPTER 5 CONCLUSIONS

5.1 Conclusions

The mortality and morbidity associated with AKI has become a clinical problem worldwide. A conventional diagnosis, such as the measurement of serum creatinine, is not sufficiently sensitive and early enough. Thus, several biomarkers have played an important role in early diagnosis of AKI. NGAL and IL-18 have been reported as the biomarkers for early detection of AKI.

The capture NGAL antibody and anti-IL18 antibody were successfully immobilized onto a modified glass slide with covalent binding method by using EDC and NHS as linkers. The immunoassays performed on this platform gave satisfactory results. The calibration curve of NGAL and IL-18 generated from this system shows a linear relationship in the range of 50 – 1000 ng/ml of NGAL concentration and 25-1000 pg/ml of IL-18 concentrations. The R^2 of NGAL (0.9903) and IL-18 (0.9891) were quite high although they were lower than those of ELISA assays. The limit of detection of NGAL was <25 ng/ml and IL-18 was 15 pg/ml in the glass slide system which were well above the cutoff for AKI diagnosis. The limits of detection of two assays were higher than that of ELISA. The coefficients of variations were within an acceptable limit, indicating good reproducibility and repeatability of this assay platform. The glass slide system for the detection of NGAL and IL-18 was validated using plasma samples from 20 healthy volunteers and 20 AKI patients. The measurements from the glass slide system were similar to those from ELISA. No interference from plasma protein was observed. The immobilized slide could be stored for at least 1 week at 4°C in dry storage condition (purged nitrogen) without any effect on the performance of the system. In addition, the total assay time could be reduced to 1 hour and still gave a linear calibration curve, albeit lower fluorescence intensity. The shorter assay time and long storage of the printed slide make it attractive and possible for commercialization.

5.2 Recommendations

Although this glass slide system has been successfully validated for a proof-of-concept study, further improvement will make the device more robust and practical for clinical applications.

There are many biomarkers which have been reported as the biomarkers for AKI, such as kidney injury molecule-1 (KIM-1), Cystatin C and etc. Since the multiplexing immunoassay technology is capable of detecting more than one analyte, this platform should be immobilized with more than two types of captured antibodies to make the system more specific and accurate for early diagnosis of AKI.

In this study, the manual pipette was used to spot the solution onto a modified glass. It was observed that the precision of each spot was quite poor and this spotting method is not suitable for mass production. Moreover, the spotting location may possibly be varied from step to step. To overcome this problem, spotting of protein solutions should be carried out using an automatic liquid dispenser or a robotic system. An automatic machine can make this platform more practical for mass production.

There are many approaches to detect the signal and to quantify the concentration of the proteins. The fluorescence detection mode is widely used because of sensitivity but the equipment to detect fluorescence in this study, a fluorescence scanner, is not suitable for common use. A fluorescence scanner is expensive and is not always available in most laboratories. An alternative to measure fluorescence intensity is to use a fluorescence plate reader. However, the location of immobilized antibody spots on glass slide should be re-designed to align with the light source of machine. Another alternative is to change the detection mode from fluorescence signal to absorbance or chemiluminescence. The measurement can be carried out using a regular microplate reader. In this case, streptavidin would be labeled with horse radish peroxidase and react with a chemiluminescent substrate to give off light which can be measured using a plate reader.

The last limitation of our system is the stability of the printed slide. The stability of the printed slide is only 1 week which is not practical for clinical use. The longer lifetime is attractive for commercialization. Addition sucrose has been reported as preservation to preserve the activity site of antibody which binding with antigen. Thus, addition of preservative can render longer shelf life of the printed slide.

REFERENCES

1. Han, W.K. and Bonventre, J.V., 2004, "Biologic Markers for the Early Detection of Acute Kidney Injury", **Current Opinion in Critical Care**, Vol. 10, pp. 476-482.
2. Minister of Public Health, 2010, ข้อมูลสถิติการป่วยพ.ศ. 2548-2552, [online], Available: <http://bps.ops.moph.go.th/index.php?mod=bps&doc=5>
3. Naud, J.-F. and Leblanc, M., 2008, "Biomarkers in Acute Kidney Injury", **Biomarker Insights**, Vol. 3, pp. 115-125.
4. Vaidya, V.S., Ferguson, M.A., and Bonventre, J.V., 2008, "Biomarkers of Acute Kidney Injury", **Annual Review Pharmacology and Toxicology**, Vol. 48, pp. 463-493.
5. Karoonuthaisiri, N., Charlermroj, R., Uawisetwathana, U., Luxananil, P., Kirtikara, K., and Gajanandana, O., 2009, "Development of Antibody Array for Simultaneous Detection of Foodborne Pathogens", **Biosensors and Bioelectronics**, Vol. 24, pp. 1641–1648.
6. Borrebaeck, C.W.a.C.A.K., 2009, "Antibody-Based Microarrays", In **Microchip Methods in Diagnostics**, Bilitewski, U., pp 57-84.
7. Hartmann, M., Roeraade, J., Stoll, D., Templin, M.F., and Joos, T.O., 2009, "Protein Microarrays for Diagnostic Assays", **Analytical and Bioanalytical Chemistry**, Vol. 393, pp. 1407–1416.
8. Kusnezow, W. and Hoheisel, J.r.D., 2003, "Solid Supports for Microarray Immunoassays", **Journal of Molecular Recognition**, Vol. 16, pp. 165–176.
9. Lattanzio, M.R. and Kopyt, N.P., 2009, "Acute Kidney Injury: New Concepts in Definition, Diagnosis, Pathophysiology, and Treatment", **Journal of the American Osteopathic Association**, Vol. 109 No.1, pp. 13-19.
10. Santos, E.R.d., 2009, "Rifle: Association with Mortality and Length of Stay in Critically Ill Acute Kidney Injury Patients", **Revista Brasileira de Terapia Intensiva**, Vol. 21 No.4, pp. 359-368.
11. Bellomo, R., Kellum, J.A., and Ronco, C., 2004, "Defining Acute Renal Failure: Physiological Principles", **Intensive Care Medicine**, Vol. 30, pp. 33-37.
12. Nguyen, M.T. and Devarajan, P., 2008, "Biomarkers for the Early Detection of Acute Kidney Injury", **Pediatric Nephrology**, Vol. 23, pp. 2151–2157.
13. Soni, S.S., Ronco, C., Katz, N., and Cruz, D.N., 2009, "Early Diagnosis of Acute Kidney Injury: The Promise of Novel Biomarkers", **Blood Purification**, Vol. 28, pp. 165–174.

14. Devarajan, P., 2007, "Proteomics for Biomarker Discovery in Acute Kidney Injury", **Seminars in Nephrology**, Vol. 27 No.6, pp. 637-651.
15. Cowland, J.B. and Borregaard, N., 1997, "Molecular Characterization and Pattern of Tissue Expression of the Gene for Neutrophil Gelatinase-Associated Lipocalin from Humans", **Genomics**, Vol. 45, pp. 17-23.
16. Mishra, J., Ma, Q., Prada, A., Mitsnefes, M., Zahedi, K., Yang, J., Barasch, J., and Devarajan, P., 2003, "Identification of Neutrophil Gelatinase-Associated Lipocalin as a Novel Early Urinary Biomarker for Ischemic Renal Injury", **Journal of the American Society of Nephrology**, Vol. 14, pp. 2534–2543.
17. Ferguson, M.A., Vaidya, V.S., and Bonventre, J.V., 2008, "Biomarkers of Nephrotoxic Acute Kidney Injury", **Toxicology**, Vol. 245, pp. 182–193.
18. Parikh, C.R., Janib, A., Melnikov, V.Y., Faubel, S., and Edelstein, C.L., 2004, "Urinary Interleukin-18 Is a Marker of Human Acute Tubular Necrosis", **American Journal of Kidney Diseases**, Vol. 43 No.3, pp. 405-414.
19. Parikh, C.R., Abraham, E., Ancukiewicz, M., and Edelstein, C.L., 2005, "Urine IL-18 Is an Early Diagnostic Marker for Acute Kidney Injury and Predicts Mortality in the Intensive Care Unit", **Journal of the American Society of Nephrology**, Vol. 16, pp. 3046–3052.
20. Vaidya, V.S., Ramirez, V., Ichimura, T., Bobadilla, N.A., and Bonventre, J.V., 2006, "Urinary Kidney Injury Molecule-1 (Kim-1): A Sensitive Quantitative Biomarker for Early Detection of Kidney Tubular Injury", **American Journal of Physiology Renal Physiology**, Vol. 290, pp. F517–F529.
21. Han, W.K., Bailly, V., Abichandani, R., Thadhani, R., and Bonventre, J.V., 2002, "Kidney Injury Molecule-1 (Kim-1): A Novel Biomarker for Human Renal Proximal Tubule Injury", **Kidney International**, Vol. 62, pp. 237-244.
22. Lin, C.-C., Wang, J.-H., Wu, H.-W., and Lee, G.-B., 2010, "Microfluidic Immunoassays", **Journal of the Association for Laboratory Automation**, Vol. 15, No.3, pp. 253-274.
23. Bojorge Ramírez, N., Salgado, A.M., and Valdman, B., 2008, "The Evolution and Developments of Immunosensors for Health and Environmental Monitoring: Problems and Perspectives", **Brazilian Journal of Chemical Engineering**, Vol. 26, No.2, pp. 227-249.
24. Fu, Q., Zhu, J., and Van Eyk, J.E., 2010, "Comparison of Multiplex Immunoassay Platforms", **Clinical Chemistry**, Vol. 52 No.2, pp. 314–318.
25. Seurnyck-Servoss, S.L., Baird, C.L., Rodland, K.D., and Zangar, R.C., 2007, "Surface Chemistries for Antibody Microarrays", **Frontiers in Bioscience**, Vol. 12, pp. 3956-3964.

26. Jung, Y., Jeong, J.Y., and Chung, B.H., 2008, "Recent Advances in Immobilization Methods of Antibodies on Solid Supports", **Analyst**, Vol. 133, pp. 697–701.
27. Qin, M., Hou, S., Wang, L., Feng, X., Wang, R., Yang, Y., Wang, C., Yu, L., Shao, B., and Qiao, M., 2007, "Two Methods for Glass Surface Modification and Their Application in Protein Immobilization", **Colloids and Surfaces B: Biointerfaces**, Vol. 60, pp. 243-249.
28. Yu, L., Li, C.M., and Zhou, Q., 2005, "Efficient Probe Immobilization on Poly (Dimethylsiloxane) for Sensitive Detection of Proteins", **Frontiers in Bioscience**, Vol. 10, pp. 2848-2855.
29. Danczyk, R., Krieder, B., North, A., Webster, T., HogenEsch, H., and Rundell, A., 2003, "Comparison of Antibody Functionality Using Different Immobilization Methods", **Wiley InterScience**, Vol. 84, No.2, pp. 215-223.
30. Franco, E.J., Hofstetter, H., and Hofstetter, O., 2006, "A Comparative Evaluation of Random and Sitespecific Immobilization Techniques for the Preparation of Antibody-Based Chiral Stationary Phases", **Journal of separation science**, Vol. 29, pp. 1458 – 1469.
31. Gizeli, E. and Lowe, C.R., 2002, "Immobilisation of Biomolecules", **In Biomolecular Sensors**, pp 49-86.
32. Yakovleva, J., Richard, D., Lobanova, A., Bengtsson, M., Eremin, S., Laurell, T., and Emne'us, J., 2002, "Microfluidic Enzyme Immunoassay Using Silicon Microchip with Immobilized Antibodies and Chemiluminescence Detection", **Journal of American Chemical Society**, Vol. 74, pp. 2994-3004.
33. Hermanson, G., 2008, "Zero-Length Cross-Linkers", **In Bioconjugate Techniques**, pp 221-222.
34. Maraldo, D. and Mutharasan, R., 2007, "Optimization of Antibody Immobilization for Sensing Using Piezoelectrically Excited-Millimeter-Sized Cantilever (Pemc) Sensors", **Sensors and Actuators B**, Vol. 123, pp. 474-479.
35. Hu, H. and Knechtle, S.J., 2006, "Elevation of Multiple Cytokines/Chemokines in Urine of Human Renal Transplant Recipients with Acute and Chronic Injuries: Potential Usage for Diagnosis and Monitoring", **Transplantation Reviews**, Vol. 20, pp. 165–171.
36. Jager, W.d., Bourcier, K., Rijkers, G.T., Prakken, B.J., and Seyfert-Margolis, V., 2009, "Prerequisites for Cytokine Measurements in Clinical Trials with Multiplex Immunoassays", **Biomed central immunology**, Vol. 10.
37. Liu, B.-C., Zhang, L., Lv, L.-l., Wang, Y.-l., Liu, D.-g., and Zhang, X.-l., 2006, "Application of Antibody Array Technology in the Analysis of Urinary Cytokine Profiles in Patients with Chronic Kidney Disease", **American journal of nephrology**, Vol. 26, pp. 483–490.

38. Vigh-Conrad, K.A., Conrad, D.F., and Preuss, D., 2010, "A Protein Allergen Microarray Detects Specific Ige to Pollen Surface, Cytoplasmic, and Commercial Allergen Extracts", **Plos one**, Vol. 5 No.4, pp. 1-11.
39. Schulte-Pelkum, J., Hentschel, C., Kreutzberger, J., Hiepe, F., and Schoessler, W., 2005, "A Chip for the Detection of Antibodies in Autoimmune Diseases", **Autoimmunity**.
40. Ingvarsson, J., Wingren, C., Carlsson, A., Ellmark, P., Wahren, B., Engström, G., Harmenberg, U., Krogh, M., Peterson, C., and Borrebaeck, C.A.K., 2008, "Detection of Pancreatic Cancer Using Antibody Microarray-Based Serum Protein Profiling", **Proteomics**, Vol. 8, pp. 2211–2219.
41. Wen, X., He, H., and Lee, L.J., 2009, "Specific Antibody Immobilization with Biotin-Poly(L-Lysine)-G-Poly(Ethylene Glycol) and Protein a on Microfluidic Chips", **Journal of Immunological Methods**, Vol. 350, pp. 97-105.
42. Beyer, N.H., Hansen, M.Z., Schou, C., Højrup, P., and Heegaard, N.H.H., 2009, "Optimization of Antibody Immobilization for on-Line or Off-Line Immunoaffinity Chromatography", **The Journal of Separation Science**, Vol. 32, pp. 1592 – 1604.
43. Darain, F., Gan, K.L., and Tjin, S.C., 2009, "Antibody Immobilization on to Polystyrene Substrate—on-Chip Immunoassay for Horse Igg Based on Fluorescence", **Biomed Microdevices**, Vol. 11, pp. 653–661.
44. Guan, X., Zhang, H.-j., Bi, Y.-n., Zhang, L., and Hao, D.-l., 2010, "Rapid Detection of Pathogens Using Antibody-Coated Microbeads with Bioluminescence in Microfluidic Chips", **Biomed Microdevices**, Vol. 12, No.4, pp. 683-691.
45. Cras, J.J., Rowe-Taitt, C.A., Nivens, D.A., and Ligler, F.S., 1999, "Comparison of Chemical Cleaning Methods of Glass in Preparation for Silanization", **Biosensors & Bioelectronics**, Vol. 14, pp. 683-688.
46. B. DeSilva, W. Smith, R. Weiner, M. Kelley, J. Smolec, B. Lee, M. Khan, R. Tacey, Hill, H., and Celniker, A., 2003, "Recommendations for the Bioanalytical Method Validation of Ligand-Binding Assays to Support Pharmacokinetic Assessments of Macromolecules", **Pharmaceutical Research**, Vol. 20, pp. 1885-1900.
47. Bonham, M. and Miller, S., 2009, "Clinical Comparison of 99th Percentile and 10% Coefficient of Variation Cutoff Values for Four Commercially Available Troponin I Assays", **LABMEDICINE**, Vol. 40 No.8, pp. 470-473.
48. Yao, C., Zhu, T., Qi, Y., Zhao, Y., Xia, H., and Fu, W., 2010, "Development of a Quartz Crystal Microbalance Biosensor with Aptamers as Bio-Recognition Element", **Sensors**, Vol. 10, pp. 5859-5871.

49. Park, J.-W., Kurosawa, S., Aizawa, H., Wakida, S.-i., Yamada, S., and Ishihara, K., 2003, "Comparison of Stabilizing Effect of Stabilizers for Immobilized Antibodies on Qcm Immunosensors", **Sensors and Actuators B**, Vol. 91, pp. 158-162.
50. Wu, P. and Grainger, D.W.G., 2006, "Comparison of Hydroxylated Print Additives on Antibody Microarray Performance", **Journal of Proteome Research**, Vol. 5, pp. 2956-2965.
51. Kusnezow, W., Jacob, A., Walijew, A., Diehl, F., and Hoheisel, J.D., 2003, "Antibody Microarrays: An Evaluation of Production Parameters", **Proteomics**, Vol. 3, pp. 254-264.
52. Flounders, A.W., Brandon, D.L., and Bates, A.H., 1997, "Patterning of Immobilized Antibody Layers Via Photolithography and Oxygen Plasma Exposure", **Biosensors & Bioelectronics**, Vol. 12 No. 6, pp. 447-456.
53. WANG, W., SINGH, S., L. ZENG, D., KING, K., and NEMA, S., 2007, "Antibody Structure, Instability, and Formulation", **Journal of Pharmaceutical Sciences**, Vol. 96, pp. 1-26.

APPENDIX A

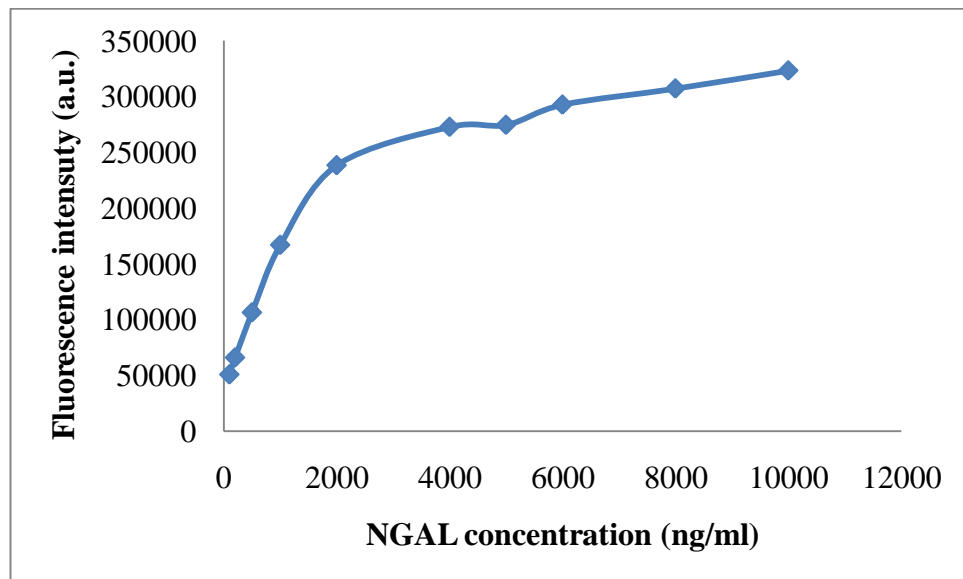
THE DATA OF NGAL AND IL-18

TableA.1 Mean fluorescence intensity, standard deviation and % of standard deviation of calibration curve of NGAL

NGAL concentration (ng/ml)	Mean fluorescence intensity (a.u.)	SD	%SD
50	32,430.81	1387.21995	4.27747529
100	49,295.27	765.562188	1.55301358
200	62,487.38	742.237712	1.18782012
500	107,722.63	1311.27909	1.21727356
1000	166,982.12	496.424246	0.29729186

TableA. 2 Mean fluorescence intensity, standard deviation and % of standard deviation of calibration curve of IL-18

IL-18 concentration (pg/ml)	Mean fluorescence intensity (a.u.)	SD	%SD
25	12172.06	22.72	2.94
50	15172.06	92.96	75.26
100	17234.84	141.27	124.98
200	19990.10	205.79	191.40
500	31295.27	470.51	463.91
1000	54222.63	1007.39	1016.58



FigureA.1 The graph of NGAL at 100-10,000 ng/ml



FigureA.2 Spot morphology

TableA.3 Fluorescence intensity and absorbance obtained by glass slide system ELISA method for NGAL detection

Sample	Fluorescence intensity (a.u.)					Absorbance 450 nm			
	1 st	2 nd	3 rd	mean	SD	1 st	2 nd	mean	SD
H1	33,565.17	33,467.28	33,979.74	33,670.73	272.05	0.0561	0.0570	0.0565	0.0006
H2	32,643.39	33,800.27	34,980.19	33,807.95	1,168.42	0.0487	0.0590	0.0538	0.0073
H3	32,073.92	32,937.25	32,801.82	32,604.33	464.31	0.0402	0.0500	0.0451	0.0069
H4	34,854.58	35,081.28	34,500.68	34,812.18	292.61	0.0631	0.0698	0.0664	0.0047
H5	33,810.41	33,621.53	33,935.86	33,789.27	158.23	0.0626	0.0568	0.0597	0.0041
H6	34,037.01	34,398.08	35,123.43	34,519.51	553.30	0.0635	0.0701	0.0668	0.0047
H7	35,716.41	35,906.58	36,177.16	35,933.38	231.54	0.0763	0.0772	0.0768	0.0006
H8	30,693.07	30,773.87	31,559.36	31,008.77	478.54	0.0229	0.0337	0.0283	0.0076
H9	33,311.21	32,907.22	32,739.13	32,985.85	256.01	0.0712	0.0765	0.0738	0.0037
H10	28,900.20	29,860.69	28,454.56	29,071.82	1,811.46	0.0312	0.0346	0.0329	0.0024
H11	31,980.40	32,672.87	32,685.81	32,446.36	870.84	0.0713	0.0681	0.0697	0.0023
H12	31,702.03	31,048.00	31,055.43	31,268.49	1,464.27	0.0559	0.0564	0.0562	0.0004
H13	30,283.02	32,114.59	31,016.78	31,138.13	1,744.55	0.0477	0.0498	0.0487	0.0015
H14	31,109.56	31,332.46	31,175.61	31,205.88	93.73	0.0598	0.0541	0.0569	0.0040
H15	32,681.24	30,499.88	31,324.90	31,502.01	2,015.76	0.0531	0.0594	0.0562	0.0045
H16	32,173.66	30,070.32	30,552.98	30,932.32	839.68	0.0455	0.0537	0.0496	0.0058
H17	21,277.77	22,383.25	25,012.15	22,891.06	1,918.28	0.0378	0.0472	0.0425	0.0066
H18	29,286.52	30,365.36	26,924.07	28,858.65	1,760.09	0.0823	0.0949	0.0886	0.0089
H19	25,768.10	25,479.03	25,862.14	25,703.09	199.66	0.0640	0.0751	0.0695	0.0078
H20	28,521.99	27,477.70	26,059.53	27,353.07	1,235.95	0.0645	0.0772	0.0708	0.0090
2	53,288.32	51,513.17	51,681.04	52,160.84	980.02	0.0206	0.0239	0.0223	0.0023
3	70,122.56	69,740.28	70,813.24	70,225.36	543.82	0.0455	0.0436	0.0445	0.0013
B12	54,732.28	54,711.77	56,581.45	55,341.83	1,073.59	0.0302	0.0286	0.0294	0.0011
B13	33,434.28	36,140.38	34,093.80	34,556.15	1,411.05	0.0047	0.0026	0.0037	0.0015
B15	51,287.58	51,549.93	51,300.90	51,379.47	147.77	0.0439	0.0420	0.0430	0.0013

B23	39,729.30	39,844.17	39,706.77	39,760.08	73.69	0.0209	0.0213	0.0211	0.0003
B24	45,159.87	45,267.28	45,135.17	45,187.44	70.24	0.0298	0.0311	0.0304	0.0009
B27	62,627.35	62,289.21	62,190.04	62,368.87	229.28	0.0568	0.0629	0.0598	0.0043
B28	43,032.25	42,740.04	43,198.71	42,990.33	232.19	0.0238	0.0267	0.0253	0.0021
B29	77,821.56	77,326.33	77,288.83	77,478.91	297.34	0.0838	0.0834	0.0836	0.0003
B30	40,946.07	41,053.05	40,782.21	40,927.11	136.41	0.0217	0.0242	0.0230	0.0018
B31	40,228.15	40,936.66	40,104.19	40,423.00	449.14	0.0180	0.0213	0.0196	0.0023
B32	98,770.55	97,793.47	98,208.39	98,257.47	490.39	0.0824	0.0840	0.0832	0.0011
B33	116,778.95	117,636.14	118,281.58	117,565.56	753.80	0.0894	0.1083	0.0988	0.0134
B34	52,693.92	53,638.64	53,717.20	53,349.92	569.47	0.0153	0.0198	0.0175	0.0032
B35	73,901.34	73,336.31	73,375.16	73,537.60	315.60	0.0424	0.0420	0.0422	0.0003
B37	100,607.62	99,916.25	100,384.09	100,302.65	352.81	0.0761	0.0776	0.0768	0.0011
B40	58,779.08	58,613.66	58,353.12	58,581.95	214.74	0.0222	0.0284	0.0253	0.0044
B41	61,336.72	61,779.82	61,647.12	61,587.89	227.41	0.0259	0.0316	0.0288	0.0040
B43	76,203.27	75,828.27	75,940.16	75,990.57	192.51	0.0444	0.0467	0.0455	0.0016

TableA.4 Fluorescence intensity and absorbance obtained by glass slide system ELISA method for IL-18 detection

Sample	Fluorescence intensity (a.u.)					Absorbance 450 nm			
	1 st	2 nd	3 rd	mean	SD	1 st	2 nd	mean	SD
H1	24,706.92	24,184.99	24,336.15	24,409.35	268.55	0.0916	0.0952	0.0934	0.0025
H2	23,098.78	21,887.46	22,617.37	22,534.54	609.89	0.0839	0.0861	0.0850	0.0016
H3	30,773.28	31,951.88	31,293.27	31,339.48	590.66	0.1320	0.1251	0.1286	0.0049
H4	38,102.08	38,933.15	36,947.93	37,994.39	996.98	0.1753	0.1745	0.1749	0.0006
H5	20,360.91	21,358.88	25,246.90	22,322.23	2,581.52	0.0747	0.0780	0.0763	0.0023
H6	18,111.01	14,967.04	14,115.36	15,731.14	2,104.56	0.0491	0.0588	0.0539	0.0069
H7	21,321.77	20,334.89	21,882.24	21,179.63	783.41	-	0.0700	0.0700	0.0000
H8	15,836.87	14,487.80	16,180.89	15,501.85	894.88	0.0487	0.0482	0.0484	0.0004
H9	16041.24	15238.57	16761.96	16,013.92	762.06	0.0425	0.0450	0.0438	0.0018
H10	18408.8	17313.96	21242.11	18,988.29	2,027.18	0.0554	0.0534	0.0544	0.0014
H11	19329.78	20814.71	20493.16	20,212.55	781.22	0.0576	0.0612	0.0594	0.0025
H12	19894.21	20048.25	20924.41	20,288.96	555.68	0.0671	0.0597	0.0634	0.0052
H13	25394.26	23006.71	24277.15	24,226.04	1,194.60	0.0860	0.0801	0.0831	0.0042
H14	18645.02	21314.77	19876.24	19,945.34	1,336.22	0.0601	0.0621	0.0611	0.0014
H15	19439.07	17545.24	18925.25	18,636.52	979.37	0.0576	0.0586	0.0581	0.0007
H16	23167.97	23792.03	23007.09	23,322.36	414.62	0.0779	0.0731	0.0755	0.0034
H17	15,463.62	15,234.94	15,916.95	15,538.50	347.12	0.0413	0.0374	0.0394	0.0028
H18	24,301.10	23,623.33	25,061.83	24,328.75	719.65	0.0916	0.0916	0.0916	0.0000
H19	19,803.50	20,341.67	19,468.54	19,871.24	440.49	0.0584	0.0623	0.0604	0.0028
H20	25,381.68	25,859.47	26,414.89	25,885.35	517.09	0.0951	0.0974	0.0963	0.0016
2	56,408.58	55,845.53	58,230.52	56,828.21	1,246.64	0.4071	0.3884	0.3977	0.0132
3	55,440.12	54,947.88	56,904.01	55,764.00	1,017.49	0.3310	0.3449	0.3379	0.0098
B12	63,539.16	57,280.65	65,490.66	62,103.49	4,289.16	0.4382	0.4340	0.4361	0.0030
B13	22,719.01	20,209.82	20,947.90	21,292.24	1,289.55	0.0747	0.0778	0.0763	0.0022
B15	28,238.27	31,254.91	30,012.15	29,835.11	1,516.09	0.1158	0.1134	0.1146	0.0017

B23	57,393.08	54,936.41	55,884.53	56,071.34	1,238.94	0.3496	0.3480	0.3488	0.0011
B24	36,304.13	36,180.26	35,255.02	35,913.14	573.30	0.1445	0.1523	0.1484	0.0055
B27	34,168.33	34,727.98	33,466.62	34,120.98	632.01	0.1337	0.1321	0.1329	0.0011
B28	18,231.74	16,665.18	19,469.44	18,122.12	1,405.34	0.0450	0.0408	0.0429	0.0030
B29	78,957.17	79,384.76	75,053.98	77,798.64	2,386.54	0.7508	0.7181	0.7344	0.0231
B30	43,837.02	41,839.69	43,583.56	43,086.76	1,087.40	0.1966	0.1914	0.1940	0.0037
B31	39,182.35	36,963.37	36,854.14	37,666.62	1,313.80	0.1626	0.1728	0.1677	0.0072
B32	59,364.97	57,994.34	59,841.97	59,067.09	959.16	0.4510	0.4545	0.4528	0.0025
B33	56,074.42	57,640.95	58,072.70	57,262.69	1,051.47	0.4588	0.4242	0.4415	0.0245
B34	81,354.76	83,315.80	80,956.97	81,875.84	1,262.80	0.9022	0.7609	0.8316	0.0999
B35	65,912.59	65,676.22	64,369.40	65,319.40	831.17	0.5381	0.5736	0.5559	0.0251
B37	64,030.03	65,596.08	67,364.43	65,663.51	1,668.22	0.6402	0.5838	0.6120	0.0399
B40	24,990.97	27,522.39	27,650.05	26,721.14	1,499.73	0.1298	0.1162	0.1230	0.0096
B41	105,550.96	103,250.44	102,302.22	103,701.21	1,670.62	1.1766	1.2269	1.2018	0.0356
B43	56,272.14	54,267.83	56,333.91	55,624.63	1,175.43	0.4191	0.4203	0.4197	0.0008

TableA.5 Quantitative of plasma NGAL (ng/ml) obtained by glass slide system and ELISA method

Sample	GLASS					ELISA				P-value
	1 st	2 nd	3 rd	mean	SD	1 st	2 nd	mean	SD	
H1	49.2354	48.5864	51.9840	49.9352	1.8037	57.6642	54.2070	55.9356	2.4446	0.0485
H2	43.1240	50.7941	58.6169	50.8450	7.7466	52.2628	55.6962	53.9795	2.4278	0.6328
H3	39.3484	45.0723	44.1744	42.8650	3.0784	46.0584	48.9948	47.5266	2.0763	0.1641
H4	57.7841	59.2871	55.4378	57.5030	1.9400	62.7737	63.7379	63.2558	0.6818	0.0307
H5	50.8613	49.6090	51.6930	50.7211	1.0490	62.4088	54.0581	58.2334	5.9048	0.1011
H6	52.3637	54.7575	59.5666	55.5626	3.6683	63.0657	63.9613	63.5135	0.6333	0.0632
H7	63.4980	64.7589	66.5528	64.9366	1.5351	72.4088	69.2480	70.8284	2.2350	0.0371
H8	30.1934	30.7291	35.9369	32.2865	3.1727	33.4307	36.8578	35.1442	2.4233	0.3657
H9	64.3197	61.4098	60.1990	61.9762	2.1179	68.6861	68.7267	68.7064	0.0287	0.0237
H10	32.5470	39.4655	29.3370	33.7832	5.1761	39.4891	37.5279	38.5085	1.3867	0.3151
H11	54.7338	59.7217	59.8150	58.0902	2.9070	68.7591	62.4721	65.6156	4.4456	0.0996
H12	52.7287	48.0177	48.0712	49.6059	2.7046	57.5182	53.7602	55.6392	2.6573	0.091
H13	42.5075	55.7004	47.7928	48.6669	6.6397	51.5328	48.8459	50.1894	1.9000	0.7827
H14	48.4611	50.0667	48.9369	49.1549	0.8247	60.3650	52.0477	56.2063	5.8812	0.1118
H15	59.7820	44.0696	50.0122	51.2880	7.9335	55.4744	55.9940	55.7342	0.3674	0.5069
H16	56.1259	40.9754	44.4521	47.1845	7.9362	49.9270	51.7498	50.8384	1.2889	0.5828
H17	22.8662	30.8079	49.6937	34.4559	13.7807	44.3066	46.9099	45.6082	1.8408	0.3589
H18	80.4004	88.1506	63.4287	77.3266	12.6443	76.7883	82.4274	79.6079	3.9874	0.8284
H19	55.1244	53.0477	55.7999	54.6573	1.4343	63.4307	67.6843	65.5575	3.0078	0.0107
H20	74.9080	67.4060	57.2180	66.5107	8.8790	63.7956	69.2479	66.5218	3.8554	0.9988
2	252.8271	240.0746	241.2805	244.7274	7.0404	254.0146	236.4855	245.2501	12.3949	0.9542
3	373.7627	371.0165	378.7245	374.5012	3.9067	399.4161	353.8347	376.6254	32.2309	0.9097
B12	263.2004	263.0530	276.4846	267.5793	7.7126	310.0730	264.4825	287.2777	32.2373	0.3523
B13	110.1975	129.6379	114.9354	118.2569	10.1369	161.1679	109.6054	135.3866	36.4602	0.4676
B15	345.3465	347.8903	345.4756	346.2375	1.4329	390.0730	344.3038	367.1884	32.3637	0.3077

B23	233.2716	234.3854	233.0531	233.5701	0.7145	255.7664	220.9977	238.3821	24.5852	0.7353
B24	285.9291	286.9706	285.6896	286.1965	0.6811	307.7372	279.3745	293.5559	20.0555	0.5368
B27	455.3025	452.0238	451.0622	452.7961	2.2232	465.4015	468.8012	467.1013	2.4040	0.0063
B28	265.2987	262.4652	266.9127	264.8922	2.2514	272.7007	253.1645	262.9326	13.8142	0.8101
B29	602.6332	597.8312	597.4676	599.3106	2.8831	623.0657	590.9159	606.9908	22.7334	0.5729
B30	245.0700	246.1073	243.4811	244.8862	1.3227	260.4380	238.2725	249.3552	15.6733	0.6284
B31	238.1087	244.9788	236.9067	239.9981	4.3551	238.8321	220.9977	229.9149	12.6108	0.2661
B32	556.7311	549.4199	552.5246	552.8919	3.6695	614.8906	594.4900	604.6903	14.4254	0.0077
B33	691.4842	697.8984	702.7281	697.3702	5.6405	655.7664	739.2405	697.5035	59.0251	0.9969
B34	211.9494	219.0186	219.6064	216.8581	4.2612	223.0657	212.0626	217.5641	7.7804	0.9004
B35	370.6401	366.4121	366.7028	367.9183	2.3616	381.3139	344.3038	362.8088	26.1701	0.7377
B37	570.4776	565.3042	568.8049	568.1956	2.6400	578.1022	556.3663	567.2343	15.3696	0.9155
B40	257.4834	256.2456	254.2960	256.0083	1.6069	263.3577	263.2911	263.3244	0.0470	0.0088
B41	276.6217	279.9373	278.9443	278.5011	1.7017	284.9635	282.3530	283.6582	1.8459	0.0484
B43	387.8649	385.0589	385.8961	386.2733	1.4405	392.9927	372.3008	382.6468	14.6314	0.6731

TableA.6 Quantitative of plasma IL-18 (pg/ml) obtained by glass slide system and ELISA method

Sample	GLASS					ELISA				P-value
	1 st	2 nd	3 rd	mean (pg/ml)	SD	1 st	2 nd	mean	SD	
H1	346.1093	334.0275	337.5266	339.2211	6.2166	337.0833	352.0833	344.5833	10.6066	0.5137
H2	308.8838	280.8440	297.7400	295.8226	14.1179	305.0000	314.1667	309.5833	6.4818	0.3962
H3	486.5343	513.8167	498.5711	499.6407	13.6726	505.4167	476.6667	491.0417	20.3293	0.6017
H4	656.1824	675.4201	629.4660	653.6895	23.0783	685.8334	682.5000	684.1667	2.3570	0.1754
H5	245.5072	268.6083	358.6088	290.9081	59.7575	266.6667	280.4167	273.5417	9.7227	0.7243
H6	193.4262	120.6491	100.9343	138.3365	48.7167	160.0000	200.4167	180.2083	28.5789	0.3649
H7	267.7493	244.9049	280.7231	264.4591	18.1344	-	247.0833	247.0833	0.0000	0.2889
H8	140.7840	109.5556	148.7475	133.0290	20.7149	158.3333	156.2500	157.2917	1.4731	0.2146
H9	107.5611	87.1567	125.8824	106.8667	19.3722	132.5000	142.9167	137.7083	7.3657	0.1312
H10	167.7462	139.9146	239.7710	182.4772	51.5323	186.2500	177.9167	182.0833	5.8926	0.9925
H11	191.1582	228.9061	220.7321	213.5988	19.8593	195.4167	210.4167	202.9167	10.6066	0.548
H12	205.5064	209.4222	231.6948	215.5411	14.1258	235.0000	204.1667	219.5833	21.8025	0.8121
H13	345.3216	284.6283	316.9238	315.6246	30.3675	313.7500	289.1667	301.4583	17.3830	0.6025
H14	173.7511	241.6180	205.0496	206.8062	33.9676	205.8333	214.1667	210.0000	5.8926	0.9083
H15	193.9364	145.7939	180.8747	173.5350	24.8964	195.4167	199.5833	197.5000	2.9463	0.2884
H16	288.7277	304.5917	284.6380	292.6525	10.5400	280.0000	260.0000	270.0000	14.1421	0.1276
H17	98.5056	92.7409	109.9334	100.3933	8.7503	127.5000	111.2500	119.3750	11.4905	0.1227
H18	321.2861	304.2005	340.4631	321.9832	18.1413	337.0833	337.0833	337.0833	0.0000	0.3455
H19	207.9079	221.4745	199.4641	209.6155	11.1041	198.7500	215.0000	206.8750	11.4905	0.8066
H20	348.5261	360.5705	374.5718	361.2228	13.0351	351.6667	361.2500	356.4583	6.7764	0.6766
2	1416.9241	1379.0771	1539.3910	1445.1307	83.7965	1651.6666	1573.7500	1612.7083	55.0954	0.0931
3	1351.8263	1318.7390	1450.2259	1373.5971	68.3935	1334.5833	1392.4999	1363.5416	40.9532	0.8674
B12	1896.2264	1475.5428	2027.4020	1799.7237	288.3084	1781.2500	1763.7500	1772.5000	12.3744	0.9072
B13	281.4039	218.1507	236.7567	245.4371	32.5077	266.6667	279.5833	273.1250	9.1335	0.344
B15	389.6712	465.2743	434.1282	429.6912	37.9964	437.9167	427.9167	432.9167	7.0711	0.9172

B23	1425.5417	1258.7843	1323.1421	1335.8227	84.0988	1412.0833	1405.4166	1408.7500	4.7140	0.3291
B24	591.8180	588.7136	565.5252	582.0189	14.3681	557.5000	590.0000	573.7500	22.9810	0.6443
B27	538.2905	552.3165	520.7042	537.1037	15.8395	512.5000	505.8333	509.1667	4.7140	0.1035
B28	138.8872	99.6261	169.9065	136.1399	35.2207	142.9167	125.4167	134.1667	12.3744	0.9464
B29	2889.3002	2918.3247	2624.3538	2810.6596	161.9969	3083.7499	2947.4999	3015.6249	96.3433	0.2156
B30	780.6075	730.5504	774.2553	761.8044	27.2525	774.5833	752.9166	763.7500	15.3206	0.9347
B31	663.9520	608.3399	605.6024	625.9648	32.9264	632.9167	675.4166	654.1666	30.0520	0.4055
B32	1831.2123	1736.3196	1864.2364	1810.5894	66.4052	1834.5834	1849.1666	1841.8750	10.3119	0.5744
B33	1603.3980	1711.8534	1741.7447	1685.6653	72.7964	1867.0833	1722.9167	1795.0000	101.9412	0.2476
B34	3353.6292	3489.3977	3326.0890	3389.7053	87.4274	3714.5834	3125.8333	3420.2084	416.3092	0.9024
B35	2284.5230	2268.1584	2177.6835	2243.4550	57.5445	2197.4999	2345.4168	2271.4583	104.5930	0.7153
B37	2154.1879	2262.6101	2385.0381	2267.2787	115.4959	2622.9166	2387.9166	2505.4166	166.1701	0.1478
B40	413.8983	474.7644	477.8339	455.4988	36.0598	496.2500	439.5833	467.9167	40.0694	0.7405
B41	5028.8023	4869.5306	4803.8826	4900.7385	115.6619	4857.9167	5067.5001	4962.7084	148.1978	0.6312
B43	1617.0867	1478.3225	1621.3632	1572.2575	81.3782	1701.6666	1706.6667	1704.1667	3.5356	0.118

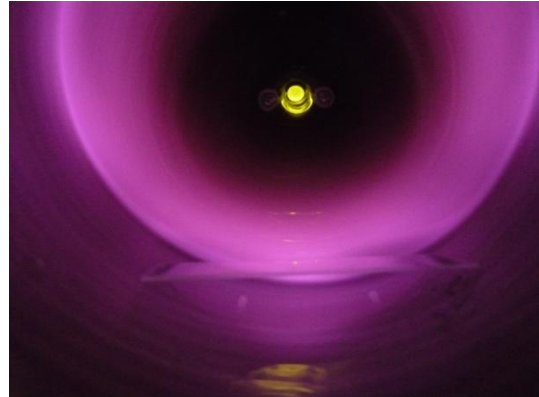
APPENDIX B
MICROFLUIDIC STUDY

B.1 Oxygen plasma treatment

Glass slides were placed inside an oxygen plasma chamber. The chamber was vacuumed for 1½ minutes before oxygen plasma was generated as shown in purple glow. The slides were exposed to oxygen plasma for 4 minutes. The chamber was vented before removing the slides.



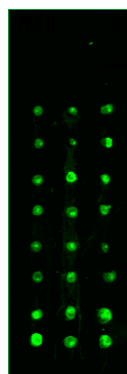
Plasma Cleaner



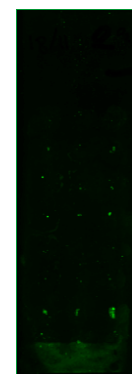
Oxygen plasma treat

FigureB.1 Oxygen plasma treat

To perform an immunoassay in a microfluidic system, slides immobilized with antibody must undergo oxygen plasma treatment. The effect of oxygen plasma treatment on the quality of immobilized antibody has not been reported. To investigate the effect of the oxygen plasma treatment on the immobilized antibody, the fluorescence signals from the antibody-immobilized slides treated with oxygen plasma were compared with the non-treated slides. The result shows that the fluorescence intensity of the non-plasma treated slide was higher than the plasma treated slide and the spot could see more clearly as shown in Figure 4.5. The surface of the glass slide was oxidized by oxygen plasma, causing the oxidization of the antibody leading to denaturation. Thus, the activity of immobilized antibody is decreased. Moreover, oxygen plasma treatment could clean the surface and made the surface to be more hydrophilic which can removed the antibody that is previously immobilized [52].



A.



B.

FigureB.2 Fluorescence image A. non-oxygen plasma treat and B. Oxygen plasma treat

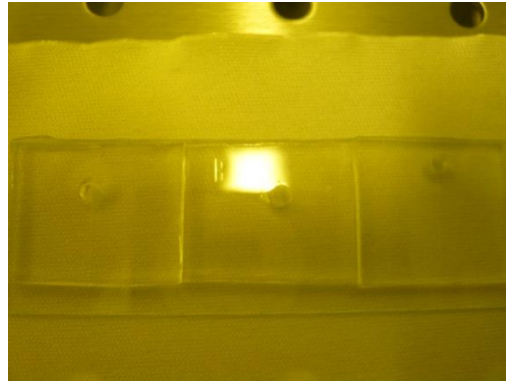
B.2 Power free testing

Air in PDMS was evacuated in vacuum desiccators at 10 kPA for 1 hour. Immediately after removal from the desiccators, the chip was covered with adhesive tape (Scotch, USA), and was placed on a stage of microscope.



FigureB.3 Evacuated the air in PDMS

The width of channels is 500 μ m. Middle chip was tested with DI water. The result showed that DI water was introduced into the channel and filled full channel. Air dissolved in PDMS was evacuated in a vacuum. When the microchip is brought back to the atmosphere, air dissolves into PDMS again and drives the solution into the channel. Right chip was used on next day and kept in the seal box at room temperature to test the storage time. The methylene blue is a sample. It could flow into the channel like DI water but couldn't fill full channel. The surface of chip turned to hydrophobic when time pass for a while. Therefore, the fluid flow is difficult. Another chip was treated with oxygen plasma and test capillary force without evacuated air in PDMS. The red water is sample. The result showed that the red water flowed into channel and filled full channel because of a hydrophilicity surface due to oxygen plasma.



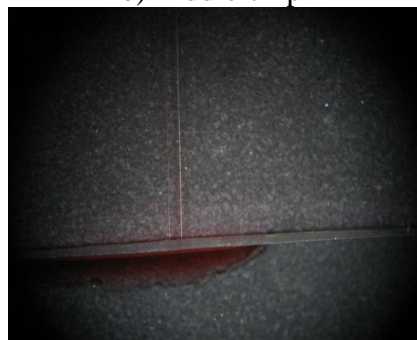
a)Micro chip



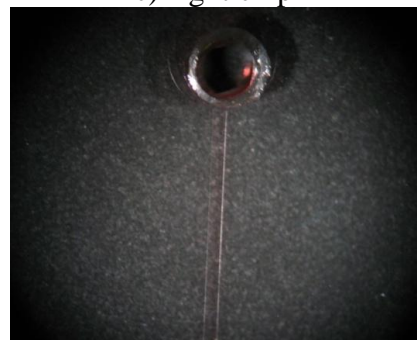
b)Middle chip



c)Right chip



d)Left chip



e)Filled channel with red water

FigureB.4 Power free testing of each micro chip

APPENDIX C
THE CONSENT FORM

หนังสือแสดงเจตนายินยอมเข้าร่วมการวิจัย

โครงการวิจัยเรื่อง การวินิจฉัยโรคไตวายเฉียบพลัน โดยใช้เทคโนโลยี Multiplexing Immunoassay

วันที่ให้คำยินยอม วันที่เดือนพ.ศ.....

ข้าพเจ้า.....เลขบัตรประชาชน.....

ก่อนที่จะลงนามในใบยินยอมให้ทำการวิจัยนี้ ข้าพเจ้าได้รับการอธิบายจากผู้วิจัยถึงวัตถุประสงค์ของการวิจัย วิธีการวิจัย อันตรายหรืออาการที่อาจเกิดขึ้นจากการวิจัยหรือ รวมทั้งประโยชน์ที่จะเกิดขึ้นจากการวิจัยอย่างละเอียด และมีความเข้าใจดีแล้ว ซึ่งผู้วิจัยได้ตอบคำถามต่างๆ ที่ข้าพเจ้าสงสัยด้วยความเต็มใจ ไม่ปิดบัง ซ่อนเร้น จนข้าพเจ้าพอใจ และเข้าร่วมโครงการนี้โดยสมัครใจ

ผู้วิจัยรับรองว่าจะเก็บข้อมูลเฉพาะเกี่ยวกับตัวข้าพเจ้าเป็นความลับ และจะเปิดเผยได้เฉพาะในรูปแบบที่เป็นสรุปผลการวิจัย โดยการตกลงที่จะเข้าร่วมการศึกษานี้ข้าพเจ้าได้ให้คำยินยอมที่จะให้มีการตรวจสอบข้อมูลประวัติทางการแพทย์ของผู้เข้าร่วมวิจัยได้

การเปิดเผยข้อมูลเกี่ยวกับตัวข้าพเจ้าต่อหน่วยงานต่างๆ ที่เกี่ยวข้องกระทำได้เฉพาะกรณีจำเป็น ด้วยเหตุผลทางวิชาการเท่านั้นและจะต้องได้รับคำยินยอมจากข้าพเจ้าเป็นลายลักษณ์อักษร

ในการวิจัยครั้งนี้ ผู้วิจัยได้ขอความอนุเคราะห์จากงานพยาบาล มหาวิทยาลัยพระจอมเกล้าธนบุรี ในการเจาะเลือดอาสาสมัคร คนละ 2 ซีซี จำนวน 1 ครั้ง เพื่อใช้ในการตรวจหาโปรตีนในเลือดเท่านั้น และจะมีการเก็บปัสสาวะ เพื่อตรวจหาโปรตีนในปัสสาวะ จำนวน 1 ครั้ง

ข้าพเจ้าจะไม่ได้รับค่าตอบแทนใดๆ จากการเข้าร่วมการวิจัยนี้

ข้าพเจ้าได้อ่านข้อความข้างต้นและมีความเข้าใจดีทุกประการแล้ว ยินดีเข้าร่วมในการวิจัยด้วยความเต็มใจ จึงได้ลงนามในเอกสารแสดงความยินยอมนี้

ลงนาม.....ผู้ยินยอม

(.....)

ลงนาม.....พยาน

(.....)

ลงนาม.....พยาน

(.....)

CURRICULUM VITAE

NAME	Miss Thanaporn Bovornvirakit
DATE OF BIRTH	26 January 1987
EDUCATIONAL RECORD	
HIGH SCHOOL	Assumption Convent School, 2005
BACHELOR'S DEGREE	Bachelor of Science (Biotechnology) Silapakorn University, 2009
MASTER'S DEGREE	Master of Science (Biological Engineering) King Mongkut's University of Technology Thonburi, 2011
SCHOLARSHIP/ RESEARCH GRANT	<ul style="list-style-type: none">• KMUTT Diamond Scholarship, Academic Year 2010.• Higher Education Research Promotion and National Research University (NRU) Project of Thailand by Office of the Higher Education Commission.• National Research Council of Thailand (NRCT), Academic Year 2012.
PUBLICATION	T. Bovornvirakit and K. Viravaidya-Pasuwat, 2011 "Development of An Immunoassay Platform for Diagnosis of Acute Kidney Injury" WASET 2011 Bali, Indonesia International Conference Program (WASET 2011) , October, 26-28, Indonesia.

King Mongkut's University of Technology Thonburi
Agreement on Intellectual Property Rights Transfer for Postgraduate Students

Date..... 19 December 2011.....

Name Miss Thanaporn Middle Name -
Surname/Family Name Bovornvirakit
Student Number 52401205 who is a student of King's Mongkut's University
of Technology Thonburi (KMUTT) in Graduate Diploma Master Degree
 Doctoral Degree
Program Master of Science Field of Study Biological Engineering
Faculty/School Faculty of Engineering
Home Address 17/28 Soi Charoen Nakhon 57 Charoen Nakhon Rd. Bukkalo Thonburi
Bangkok
Postal Code 10600 Country Thailand

I, as 'Transferer', hereby transfer the ownership of my thesis copyright to King's Mongkut's University of Technology Thonburi who has appointed **Assoc. Prof. Dr. Piyabutr Wanichpongpan Associate Dean for Academic Affairs (Acting for Dean)** to be 'Transferee' of copyright ownership under the 'Agreement' as follows.

1. I am the author of the thesis entitled Multiplexing Immunoassay for the Diagnosis of Acute Kidney Injury under the supervision of Asst. Prof. Dr. Kwanchanok Pasuwat who is my supervisor, and/or who is/are my co-supervisor(s), in accordance with the Thai Copyright Act B.E. 2537. The thesis is a part of the curriculum of KMUTT.
2. I hereby transfer the copyright ownership of all my works in the thesis to KMUTT throughout the copyright protection period in accordance with the Thai Copyright Act B.E. 2537, effective on the approval date of thesis proposal consented by KMUTT.
3. To have the thesis distributed in any form of media, I shall in each and every case stipulate the thesis as the work of KMUTT.
4. For my own distribution of thesis or the reproduction, adjustment, or distribution of thesis by the third party in accordance with the Thai Copyright Act B.E. 2537 with remuneration in return, I am subject to obtain a prior written permission from KMUTT.
5. To use any information from my thesis to make an invention or create any intellectual property works within ten (10) years from the date of signing this Agreement, I am subject to obtain prior written permission from KMUTT, and KMUTT is entitled to have intellectual property rights on such inventions or intellectual property works, including entitling to take royalty from licensing together with the distribution of any benefit deriving partly or wholly from the works in the future, conforming with the Regulation of King Mongkut's Institute of Technology Thonburi *Re* the Administration of Benefits deriving from Intellectual Property B.E. 2538.

6. If the benefits arise from my thesis or my intellectual property works owned by KMUTT, I shall be entitled to gain the benefits according to the allocation rate stated in the Regulation of King Mongkut's Institute of Technology Thonburi *Re* the Administration of Benefits deriving from Intellectual Property B.E. 2538.

Signature.....Transferor
(Miss Thanaporn Bovornvirakit)
Student

Signature.....Transferee
(Assoc. Prof. Dr. Piyabutr Wanichpongpan)
Associate Dean for Academic Affairs (Acting for Dean)

Signature.....Witness
(.....)

Signature.....Witness
(.....)